EVALUATION OF A SINGLE-PHOTON COMPTON SCATTERING METHOD FOR THE IN VIVO MONITORING OF SKELETAL MINERALIZATION

by

George Edward Dyck

A thesis submitted in partial fulfillment for the requirements for the degree of

MASTER OF SCIENCE

(Physiology)

at the

University of Manitoba

1980

EVALUATION OF A SINGLE-PHOTON COMPTON SCATTERING METHOD FOR THE IN VIVO MONITORING OF SKELETAL MINERALIZATION

BY

GEORGE EDWARD DYCK

A thesis submitted to the Faculty of Graduate Studies of the University of Manitoba in partial fulfillment of the requirements of the degree of

MASTER OF SCIENCE

To Mard, disly.

ABSTRACT

EVALUATION OF A SINGLE PHOTON
COMPTON SCATTERING METHOD FOR
IN VIVO MONITORING OF SKELETAL
MINERALIZATION

by

George Edward Dyck

Under the Supervision of Dr.J.B.Sutherland, Dr.D.Cormack, and Dr.W.J.Dubé.

A simple, sensitive, in vivo method of assessing bone mineral status as an aid to early diagnosis and subsequent clinical management of patients with conditions involving potentially pathological changes in skeletal mineralization. Many methods including roentgenologic, absorptiometric and Compton scattering techniques, neutron activation analysis, and computerized tomography, each with variations, are being proposed. This thesis examines one such method employing a single phanton Compton scattering technique.

A prototype Bone Densitometer based on the theory by Clarke-1973, and built by Atomic Energy of Canada, Ltd.-Commercial Products Division, was evaluated under laboratory and clinical conditions. The instrument's ability to measure absolute density at a point, independent of surroundings was investigated and found to satisfactory only under limited circumstances. Measurements were undertaken on excised cadaver bone specimens and compared to bone mineral assays by ashing and absorptiometry. Although some correlation was found, in the main the Densitometer was an order of magnitude less sensitive than absorptiometry in measuring trabecular bone mass. Clinical studies in children and adults corroborated the findings of these in vitro experiments.

TABLE OF CONTENTS

CHAPTER ONE

INTRODUCTION

The loss of skeletal bone mineral mass is a normal consequence of ageing (Goldsmith-1971, Mazess and Cameron-1973), but accelerated loss may occur for a variety of reasons (Griffiths-1976). This phenomenon is more pronounced in women than men in later years due to the imbalance in steroid homones accompanying the menopause. A number of disease states such as hyperparathyroidism and reval failure result in osteoporosis, a general decrease in the amount of skeletal bone, and others, such as alcoholism, result in osteomalacia, a decrease in the production of the organic matrix into which the inorganic hydroxyapatite crystals are incorporated. Bone Mineral is also lost due to immobilization or disuse of a limb, or of the entire body, as might occur in paraplegic or chronic bed rest. Further, iatrogenic demineralization may occur as a result of medications or surgery. For example, corticosteroids used in the treatment of rheumatoid arthritis, and gastro-intestinal by-pass surgery have been shown to lead to increased bone resorption. Although the consequences of decreased skeletal mineral are not critical until the condition becomes quite severe, it is impor-

tant to make an early diagnosis in order to prevent the painful and debilitating sequelae of vertebral collapse and fracture of the femoral neck.

Historically, osteoporosis was diagnosed from inspection of conventional radio-graphs of the spine. However, an estimated skeletal loss of approximately 20-40% must occur before changes are seen (Lachman-1955). Other techniques involving x-rays include radiodensitometry of the metacarpal bones (Shimmins-1972), and examination of proximal femoral trabecular patterns (Singh-1970). A marked improvement in sensitivity followed the developement of photon absorptiometric methods pioneered by Cameron-1963. However, new methods such as neutron activation analysis for estimating total-body calcium (Manzke-1974), and dual-photon absorptiometry (Kan-1973) were continuously sought to overcome limitations of measurement site and nonhomogeneity of tissue cover. Most recently computerized axial tomography has been applied to the problem assessing bone mineral status in vivo (Exner-1979). At the time the experiments for this thesis were being performed, interest was being shown in Compton scattering methods to measure trabecular bone density (Clarke-1973, Garnett-1973, Luther-1973). The virtue ascribed to the Compton scattering technique was that it essentially measured absolute density at sites of trabecular bone, as opposed to measuring cortical bone or mixtures of cortical

and trabecular bone.

The Commercial Products Division of Atomic Energy of Canada, Ltd., designed and built a prototype Bone Densitometer based on the single-photon Compton scattering technique proposed by Clarke-1973. It was the subject of this thesis to evaluate this instrument as a clinical instrument for the in vivo monitoring of bone mineral status.

CHAPTER TWO

Materials and Methods

2.1 The Measurement of Specific Electron Density With the A.E.C.L. Bone Densitometer

The A.E.C.L. Bone Densitometer is prototype instrument designed and built by Atomic Energy of Canada, Limited, Commercial Products Division for in vivo assessment of trabecular bone density. The theoretical basis of the instrument's measurement of specific electron density by a single photon Compton scattering method is presented and the relationship between specific electron density and physical density is discussed. A physical description of the Densitometer is included, and the technique for using the Densitometer to measure the specific electron density of bone specimens is outlined.

2.1.1 Theory of Specific Electron Density Measurement Using a Single Photon Compton Scattering Method

The specific electron density, S.E.D., of a small selected volume within an irregular non-homogeneous object may be measured using a single photon compton scattering method (Clarke-1973). S.E.D. is defined as the ratio of the unknown electron density to the electron density of water. The method involves irradiating the selected volume, and an identical volume of water, with a narrow homogeneous photon beam from two specific angles and measuring transmitted and compton scattered beam intensities in every instance. If certain assumptions regarding the energies, dimensions, intensities, and pathways of the beams are satisfied, the S.E.D. measurement of the volume in question is independent of its surroundings and may be determined to an accuracy governed only by the statistical accuracy of the intensity measurements.

First, an expression for the absolute electron density at a point, u, within a non-uniform object is derived by consideration of events along the photon beam path as indicated in figure 2.1.1. In part (i) of the figure, a radioactive source positioned at P emits a collimated homogeneous photon beam of original intensity I, which is attenuated along its path, aub, through the object, and mea-

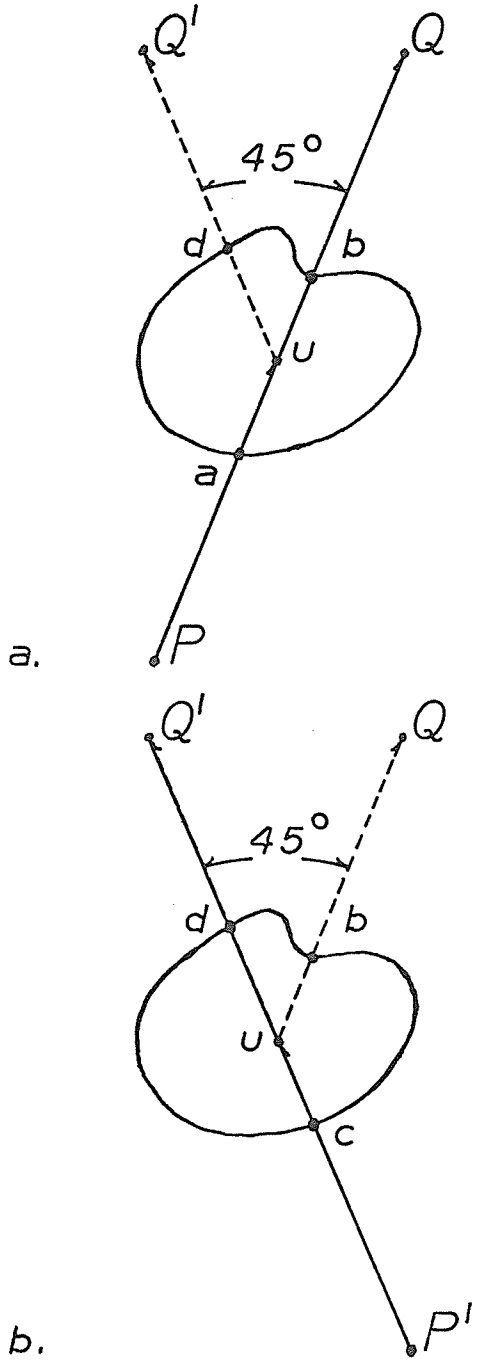

Figure 2.1.1 Single photon Compton scattering method of density measurement.

sured at Q by a collimated detector having efficiency, E. The measured countrate, T, of the transmitted beam is given by

$$T = I\ Kau\ Kub\ E \quad . \quad . \quad . \quad . \quad . \quad . \quad . \quad . \quad . \quad . \quad . \quad . \quad . \quad 2.1.1$$

where Kau and Kub are the beam transmission factors over the paths au and ub, respectively. A similar detector at Q', having an efficiency E', measures the intensity of the Compton scattered beam which originates at u, and is attenuated along the path ud. The measured countrate, S, of the scattered beam is given by

$$S = I\ Kau\ D_u\ G\ K'ud\ E' \quad . \quad . \quad . \quad . \quad . \quad . \quad . \quad . \quad . \quad . \quad . \quad 2.1.2$$

where D_u represents the electron density at U, and G is a geometry factor dependent on the Compton cross section for the original beam scattered through a 45° angle. K'ud is the transmission factor of the scattered beam over the path ud. Similarly, when the source is positioned at P', as in part (ii) of the figure, the transmitted and scattered beam countrates are given by

$$T' = I\ Kcu\ Kud\ E' \quad . \quad . \quad . \quad . \quad . \quad . \quad . \quad . \quad . \quad . \quad . \quad . \quad 2.1.3$$

$$S' = I\ Kcu\ D_u\ G\ K'_{ub}\ E \quad . \quad . \quad . \quad . \quad . \quad . \quad . \quad . \quad . \quad 2.1.4$$

It is assumed that the distance P Q equals the distance P' Q'. The expression for D_u can now be derived by multiplying eq. 2.1.2 by eq. 2.1.4, substituting from equations 2.1.1 and 2.1.3, and solving the result.

$$D_u = \frac{1}{G}\left[\frac{S\ S'}{T\ T'}\right]^{\frac{1}{2}} \quad \ldots\ldots\ldots\ldots\ldots\ldots \quad 2.1.5$$

Note that this expression for D_u depends only on G, and the measured conutrates, and is independent of any enviromental factors.

Secondly, if the same reasoning is applied to a volume of water instead of the object in question, the expression for the absolute electron density, Dw, of water becomes

$$Dw = \frac{1}{G}\left[\frac{Sw\ S'w}{Tw\ T'w}\right]^{\frac{1}{2}} \quad \ldots\ldots\ldots\ldots\ldots \quad 2.1.6$$

where Tw and Sw, and T'w and S'w, are the measured conutrates of the transmitted and scattered beams with the source at P and P', respectively.

Finally, the specific electron density, $S.E.D._u$, of the object at u is given by the ratio of equations 2.1.5 and 2.1.6.

$$S.E.D._u = \left[\frac{S\ S'\ Tw\ T'w}{Sw\ S'w\ T\ T'}\right]^{\frac{1}{2}} \quad \ldots\ldots\ldots\ldots \quad 2.1.7$$

It is this equation that the A.E.C.L. Bone Densitometer was designed to solve.

The relation between specific electron density and conventional specific gravity, S, depends on the chemical composition of the material tested (Clarke-1973). It can be shown that

$$S.E.D. = \sum_M \frac{Zi\ Ni}{Ai\ Ni}\ \frac{S}{0.55} \quad \ldots\ldots\ldots\ldots \quad 2.1.8$$

where Zi and Ai refer to the atomic number and atomic weight of the constituent elements, and Ni refers to the number of atoms per molecule of each element. The coefficient 0.55 comes from the value of Σ Zi Ni /Σ Ai Ni for water. However if the ratio of Zi/Ai can be assumed constant for the elements composing the material being measured, equation 2.1.8 simplifies to

$$S.E.D. = \frac{Z}{A} \frac{S}{0.55} \quad \ldots\ldots\ldots\ldots\ldots \quad 2.1.9$$

where the ratio Z/A is the common value for the elements in question.

Garnet-1973 notes that with the exception of hydrogen, the factor Z/A for the elements normally found in bone varies from 0.48 to 0.50, and may be assumed constant. If the proportion of hydrogen (Z/A = 1) in a material is low, therefore, specific electron density would vary directly with conventional specific gravity, and be essentially independent of chemical composition (Hazan-1977). The validity of this assumption in the present study is analyzed further in chapter three.

2.1.2 Description of the A.E.C.L. Bone Densitometer

The A.E.C.L. Bone Densitometer is a prototype instrument intended for clinical in vivo bone density measurement. It was designed and built by the Commercial Products Division of Atomic Energy of Canada, Limited, based on the theoretical considerations by Clarke-1973, for the single photon Compton scattering method of specific electron density measurement presented in 2.1.1 above. The instrument consists of a control module connected electronically to a gauge module.

The gauge module houses the radioactive source, and two NaI (T1) scintillation detectors, as represented in figure 2.1.2. The lead-shielded 153-G adolinium source can be moved laterally along a stationary tungsten support beam, by turning a hand crank. The two extremes of its travel represent the two source positions, P and P', in figure 2.1.1. Two 5mm diameter holes drilled at 45° to each other in the tungsten beam, collimate the photons emitted by the source. The two tungsten detector collimators have the same hole diameter, and are aligned along the same axis as the opposite source collimator hole. Each detector consists of a one inch diameter by $\frac{1}{2}$ inch thick Na I (T1) crystal optically coupled to a photomultiplier tube whose

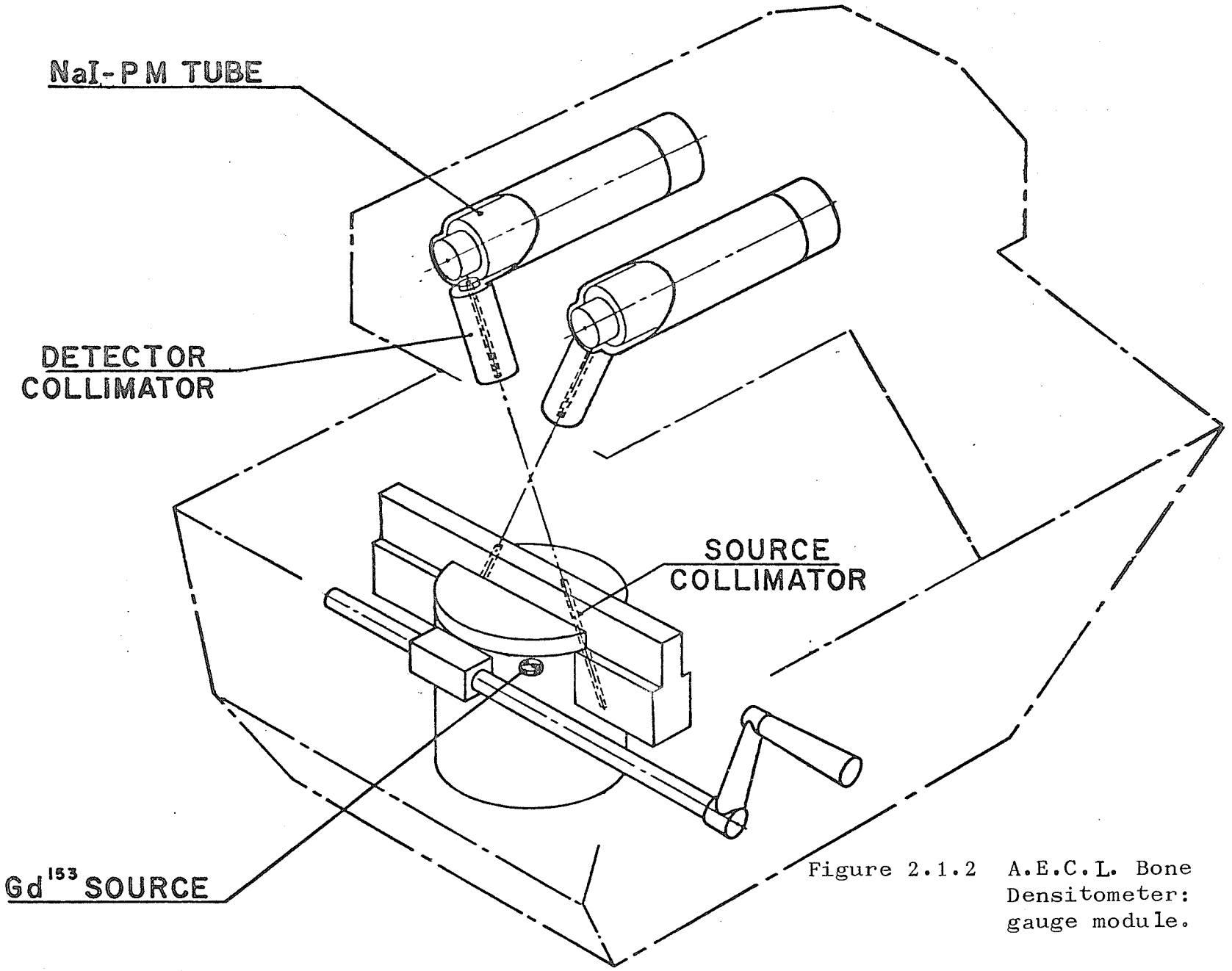

Figure 2.1.2 A.E.C.L. Bone Densitometer: gauge module.

output signal is fed to an attached preamplifier. Retractable attenuators, not shown in the diagram, are located in the detector collimators. Positioned in the path of the transmitted photon beam, they reduce its intensity by a factor of approximately 1000. Withdrawn by solenoids activated by microswitches which sense source position, they allow the less intense scattered photon beam to pass unattenuated. Power supplies also not shown in the diagram, provide high voltage to the photomultiplier tubes, and low voltage to the preamplifiers as well as to the control module. Two other gauge features not shown in figure 2.1.2, are visible in figure 2.1.3. One is the adjustable aluminum stage, used to hold and position the specimen for bone density measurement. Ball bearing and worm gear movements permit repositioning to within one millimeter along scales marked in each of the three orthogonal directions. The center of the stage has a plastic "window" to minimize photon beam attenuation. The second feature, three adjustable pointers, are attached to the gauge frame. Converging at the point in space at which the source and detector projections cross, they serve to define the point u referred to in section 2.1.1.

Data collection is initiated by a push button on the front panel of the control module. Output pulses from the two preamplifiers in the gauge are fed through separate

linear amplifiers and pulse heigh analyzers. A microprocessor routes the pulses to appropriate memory storage registers according to the position of the source and a "Standard/Sample" toggle switch. A two digit thumbwheel is used to preset the counting time in tenths of a minute increments. Depressing the "calculate" push button causes the microprocessor to calculate the specific electron density and display it on a 7 digit LED readout.

It was evident early in the study that the microprocessor computed values of S.E.D. were unreliable, so an independent method for calculating results was instituted. Unreliability stemmed mostly from failure of electronic components and at one stage from an aging source. A new source was eventually obtained, but the microprocessor boards were already obsolete and could not be replaced. Fortunately, character generator signals were provided by rear panel outputs so the contents of the eight data registers could be displayed on an external oscilloscope. S.E.D. calculations were performed manually on a calculator or automatically on a DEC-Line-8 computer using a short FOCAL program written for the purpose.

Several modifications were made to the gauge before the study was begun. The original lead attenuators were replaced by 0.5cm thick tin attenuators, which elim-

inated the lead fluorescence contribution to the transmitted beam countrate. Since the lead fluorescence contribution would be dependent on beam energy, and since there may be different degrees of beam hardening in standard and sample, countrate would not have been exactly proportional to beam intensity. This measure improved the absolute accuracy of the S.E.D. measurements of the aluminum and lucite phantoms as described in chapter three. Two other modifications to the gauge are seen in figure 2.1.3. A sheet of $\frac{1}{4}$ inch thick lead shielding has been fastened below the detectors to shield them from stray radiation. Also, the original stage was replaced, and an arm rest provided for clinical studies, by the machine shop of the Manitoba Cancer Treatment and Research Foundation.

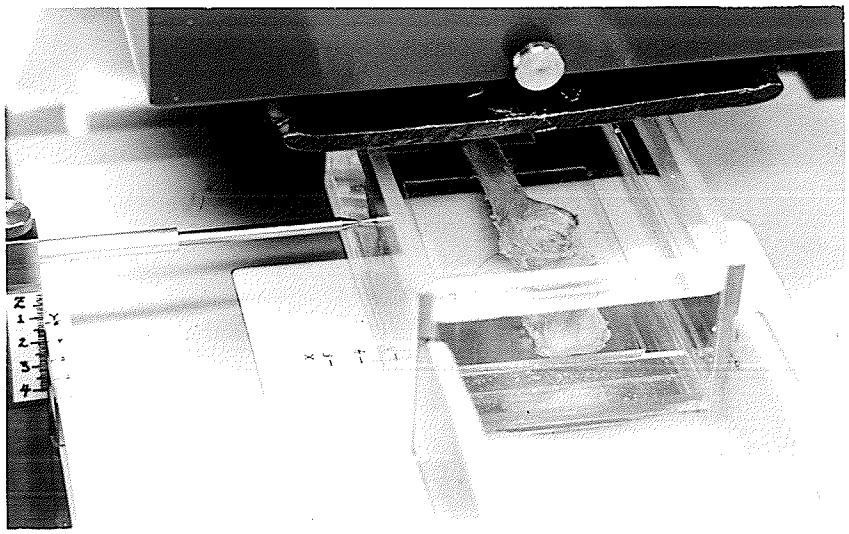

Figure 2.1.3 Distal radius in water tank on stage of A.E.C.L. Bone Densitometer in position for S.E.D. measurements.

2.1.3 Description of S.E.D. Measurement Technique For Bone Specimens

The specific electron density measurements of the mounted bone specimens were performed with the bones immersed to a uniform depth in water. For this purpose, a lucite tank, shown in figure 2.1.4, measuring 6 inches by 4 inches by 2.5 inches deep, was constructed. Bone specimens were situated in the tank with the square acrylic mounting plate fitting snuggly into the square cut out of the acrylic insert. With the bone in position, the tank was filled with water to a standard depth of 1.5 inches. The tank was placed on the gauge stage in standard orientation, as in figure 2.1.3, and adjusted in the X-direction. The stage was then adjusted to the proper Y and Z coordinates. The X and Y coordinates were based on measurements taken from x-rays of the mounted bones, and the Z coordinate was determined by inspection at the time of first measurement.

A complete S.E.D. measurement consisted of four replicate counts of the bone specimen, one count of a water standard, one count of the #1 lucite phantom (figure 3.4.1-b) and one background count. Bone specimens and the lucite phantom were counted for 2 or 3 minutes at each of the two

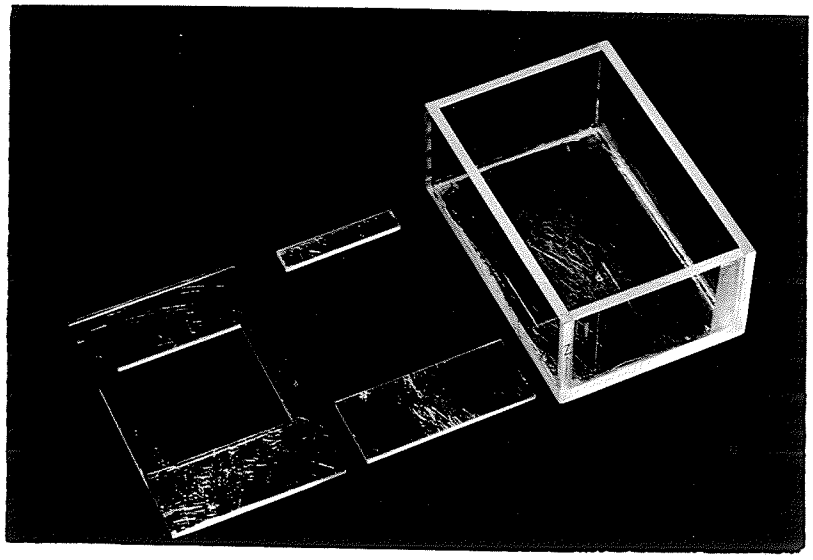

Figure 2.1.4 Lucite tank used to immerse bone specimens for S.E.D. and BMC measurements. Inserts were used to position mounted bones in standard geometry within the tank.

source positions. Transmitted counts ranged between 20 and 30 thousand, while scattered counts ranged between 2 and 3 thousand. The water standard consisted of the lucite tank filled to standard depth with water. Five to seven minutes counting times yielded 60 to 80 thousand transmitted counts and 20 to 30 thousand scattered counts. Background was taken to be the counts registered by the detectors monitoring the scattered beam with no scattering material other than air at the measurement site. Background countrates ranged between 100 and 200 counts in 2 or 3 minutes for either of the two source positions.

2.1.4 The Radioactive Source and Dosimetry Calculations

Two ^{153}Gd. sources prepared by Atomic Energy of Canada, Limited were used in the Bone Densitometer throughout the course of the study. The first source arrived with the instrument on November 1, 1972, with a specified effective strength of 1.03 Ci as of September 15, 1972. It had been prepared from a stock solution of ^{153}Gd. which was assayed at production as being greater than 99.99% pure. Trace amounts of ^{152}Eu and ^{154}Eu were the only impurities identified by solid state detector spectroscopy. The second source arrived November 12, 1974, and was labelled as having an activity of 2.5 Ci as of September 14, 1973. No exact information regarding its purity was obtained.

^{153}Gd. decays completely by electron capture to stable ^{153}Eu with a half-life of 240 days, emitting three reasonably prominent gamma rays plus Eu x-rays. Gamma ray energies are 70keV, 97keV, and 103keV, with photon yields of 2.5%, 31.7%, and 24% respectively.

The dose rate at the sensitive volume of the Bone Densitometer was calculated and measured by A.E.C.L.-CP staff (personal communication). B.J. Jackson calculated the exposure rate at the sensitive volume to be 50 mr/minute as of September 15, 1972. Two sets of measurements

using an extruded lithium fluoride thermoluminescent dosimeter (TLD) system yielded biological dose rates of 39 to 63 mrem/minute and 45 to 70 mrem/minute. The method of TLD calibration was not specified. A third set of measurements using an independent lithium fluoride chip TLD system indicated that the exposure rate was between 35 and 52 mr/minute. There was some dissatisfaction with the fact that results of the measurements exceeded the theoretical value, but no further measurements were made before shipping the source to Winnipeg.

2.2 The Measurement of Bone Mineral Content with the Norland-Cameron Bone Mineral Analyzer.

The Norland-Cameron Bone Mineral Analyzer (BMA) is a commercially available clinical instrument which measures bone mineral content (BMC) based on the direct photon absorptiometric technique developed by J.R. Cameron and J.A. Sorenson at the University of Wisconsin. The BMA is distributed by the General Electric Corporation, is widely used for clinical measurements of bone mineral content, and was used in the present study as a standard of comparison for the A.E.C.L. Bone Densitometer.

2.2.1 Theory of the Direct Photon Absorptiometric Technique for Measurement of Bone Mineral Content.

In the direct photon absorptiometric method of bone mineral content (BMC) measurement, the transmission of a narrow homogeneous photon beam through a bone is measured with a collimated NaI (Tl) scintillation detector, as in figure 2.2.1. As the beam and detector are moved in synchrony slowly across the bone, the transmission varies inversely with the amount of bone mineral in the path of the beam. Figure 2.2.2 is the plot of the log of the transmitted intensity as a function of distance travelled for a typical

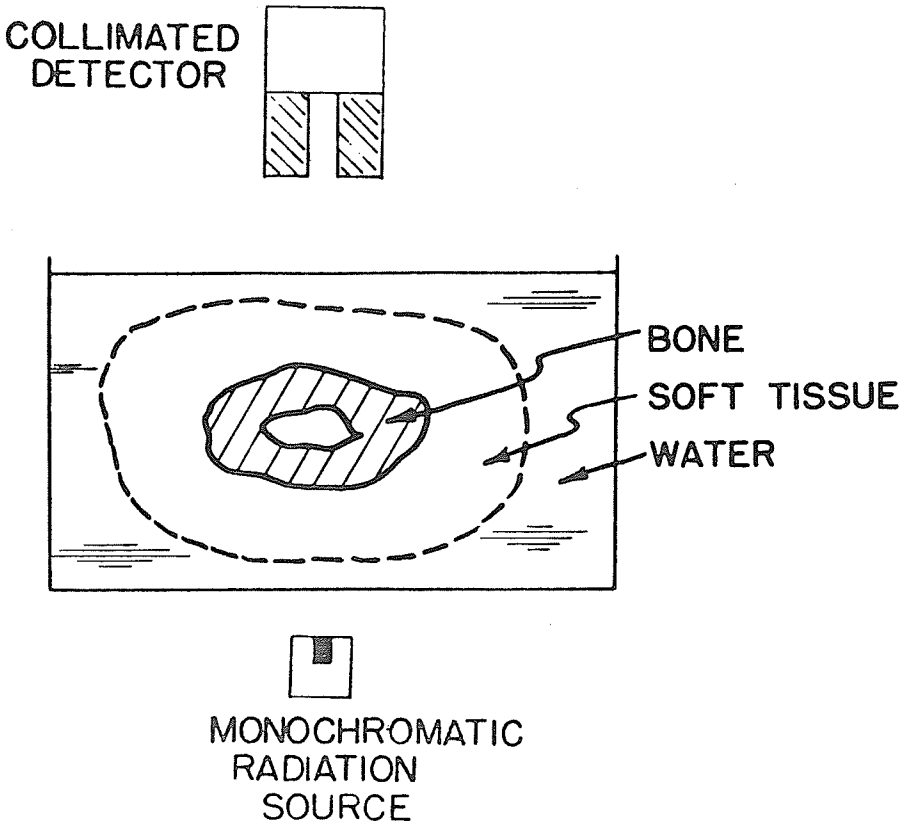

Figure 2.2.1 Physical arrangement for bone mineral content measured with the Norland-Cameron Bone Mineral Analyzer.

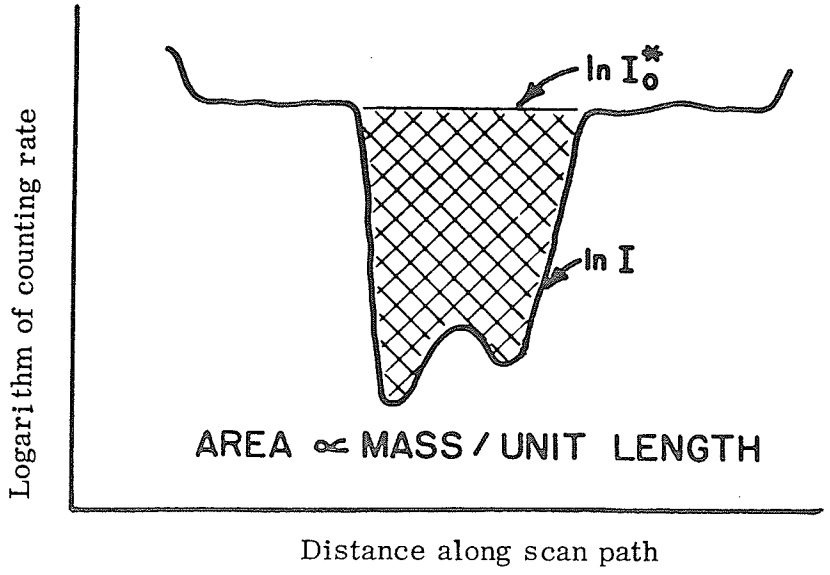

Figure 2.1.2 Typical logarithmic ratemeter tracing for scan across a long bone with Norland-Cameron Bone Mineral Analyzer.

"scan" of the diaphysis of a long bone. The total BMC encountered in the scan is found from the cross-hatched area of the transmission curve shown in figure 2.2.2, after calibration of the system against standards of known BMC. The cross-hatched area may be found by a variety of digital and analogue methods. The full mathematical treatment of the method is given by Cameron-1963.

2.2.2 Description of the Norland-Cameron Model 178 Bone Mineral Analyzer

The Norland-Cameron Model 178 Bone Mineral Analyzer (BMA) is a fully-automated instrument consisting of a scanner and a computer module. Figure 2.2.3 shows the 200mCi collimated ^{125}I source, under the measuring platform of the scanner module, and rigidly coupled to the collimated NaI (T1) scintillation detector which is situated over the platform and directly above the source. Detector output pulses are fed by cable to the linear amplifier in the computer module, after which they are analyzed by a differential discriminator. The window width is factory set at 40% of the baseline level, and the base line is adjustable on the computer module front panel. A countrate meter circuit generates an analog output signal proportional to the logarithm of the analyzed pulse rate. There is also a linear conutrate meter display with range positions of 1000, 3000, and 10,000 counts per second on the front panel of the computer module.

When the scan is initiated, a shutter opens to disclose the 1/8" diameter photon beam, and a synchronous motor drives the mechanism across the measurement platform at 1cm/sec. When the beam is attenuated by a bone specimen on the

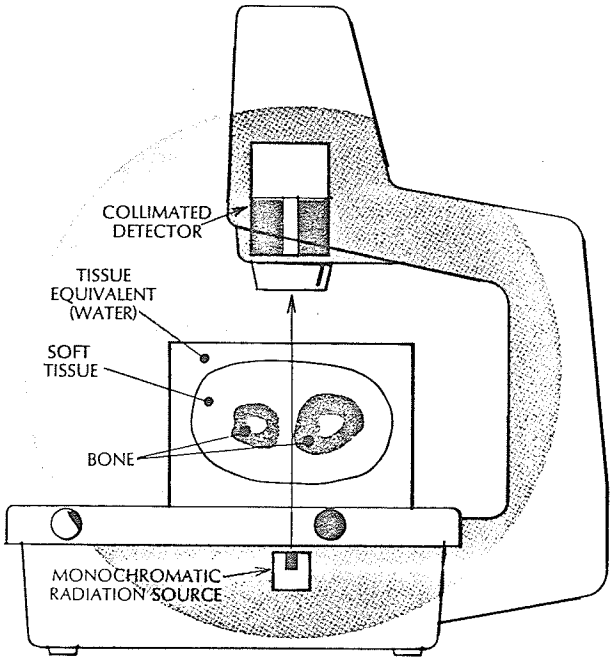

Figure 2.2.3 Norland-Cameron Bone Mineral Analyzer: Scanner Module.

platform so that its intensity falls below 70% of the unattenuated value, the mechanism backs up several millimeters, and a 10 second "zero intensity" (Io) reading is taken. Proceeding forward again, the logarithmic pulse rate signal is integrated, starting at the point where beam intensity falls below 70% of Io, and finishing where it again rises above 70% of Io. A measurement scan speed of either 1mm/sec. or 2mm/sec may be chosen. The automatic measurement cycle terminates with the mechanism in its original position, and the values for the bone mineral content (BMC) and bone width (BW) displayed on the computer module.

Three modifications were made to the BMA for the present study. First, a factory-designed "measure mode threshold" switch was installed locally to permit the selection of an 85% Io threshold when extra sensitivity in bone edge detection was desired. Second, the logarithmic pulse rate signal was fed to an external strip chart recorder to produce a hard copy tracing of the beam intensity as an aid in troubleshooting. Last, an arm rest extension was added to the measurement platform to assist in stabilizing the measured limb during clinical studies.

2.2.3 Description of the Bone Mineral Analyzer Measurement Technique for Bone Specimens.

Each mounted bone specimen was scanned with the Bone Mineral Analyzer (BMA) on the same day and under the same conditions as specific electron density (S.E.D.) measurements were made. The method of bone specimen preparation and mounting is described in section 2.3.1, and the apparatus used for a standardized water cover is described in section 2.1.3. Figure 2.2.4 shows a bone specimen in the water tank, positioned for scanning on the BMA. Each measurement consisted of four replicate scans, for which the BMC and BW values were averaged.

Scan paths were chosen by inspection of x-rays of the mounted bones, and were selected to traverse regions of predominantly trabecular bone, and in particular, to pass through the S.E.D. measurement site. Typical scan paths are illustrated in figure 2.2.5. All bone specimens were scanned in a standardized orientation.

A factory calibrated aluminum pipe phantom designed to simulate the human forearm in cross section was used for daily quality control of the BMA computer. The phantom consisted of two aluminum annuli of different dimensions embedded in a rectangular block of plastic. A hinged section of

Figure 2.2.4 Bone specimen in water tank positioned for BMC scan on Norland-Cameron Bone Mineral Analyzer.

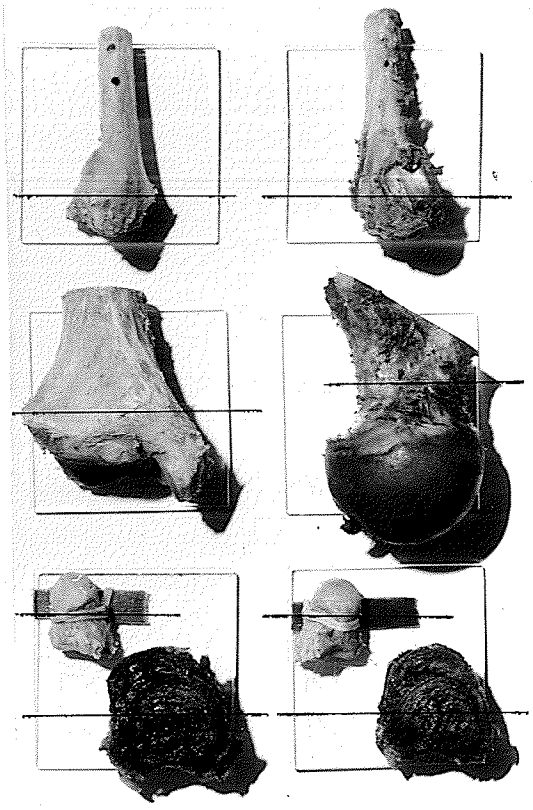

Figure 2.2.5 Mounted cadaver bones, with BMC scan paths indicated.

plastic, which could be moved into or out of the scan path, could be used to simulate high or low tissue levels, respectively. The BMA was calibrated daily by taking four replicate scans of the larger annulus with low tissue level. The BMC and BW readout values were then set to equal those printed on the phantom by adjustment of two computer module front panel controls.

2.2.4 The Radioactive Source and Densitometry Consideration

The ^{125}I source was renewed several times during the present study, but this was not thought to affect Bone Mineral Content (BMC) results because of the instrument's calibration method using the aluminum annulus phantom.

It has been estimated (Goldsmith-1971) that the exposure to the arm from one 4-scan BMC measurement is approximately 40mr, and this is highly localized to a section of tissue about 5mm wide and typically 2cm long. The major radiation, due to the scanner stopping to determine the baseline intensity, is confined to a one half cm diameter cylinder of soft tissue located just outside the bone.

2.3 Preparation of Cadaver Specimens.

Permission was obtained from the Department of Anatomy of the University of Manitoba School of Medicine to excise bones from the remains of ten cadavers. The cadavers had been partially dissected by the 1973-1974 class of first year Medical, Dental, and Medical Rehibilitation students during gross anatomy labs. Two of the cadavers were female and eight were males. The sex, age at death, and cause of death are listed in table 2.3.1. The cadavers were embalmed and had been enclosed in zippable bags at room temperature for about nine months at the time of bone excision.

Eight bones were excised from each cadaver, comprising both distal radii, both whole capitates, 8th and 9th vertebrae, one distal tibia, and one femoral neck. Nine of the tibiae and femora were from the right leg and one was from the left. The 8th vertebra from one cadaver was only partly recovered, and all other vertebra were intact. Seventy of the bones were excised between May 9 and July 18, 1974.

Five intact forearms with hands, four left and one right, were severed from their cadavers, placed in formalin-wetted plastic bags and stored at 4°C in a cold room until

April 1975, when the capitates and distal radii were excised. These bones were then prepared in the same manner as described for the bones excised between May and July 1974.

TABLE 2.3.1

CADAVER DATA

Cadaver Number	Sex	Age	Cause of Death
1161	F	41	Lympho sarcoma.
1165	F	62	Acute coronary occlusion: myocardial megaly, acute bronchitis, recurrent asthma.
1168	M	56	Cerebrovascular accident: blindness due to attempted old carotid artery surgery.
1190	M	56	Carbon monoxide poisoning.
1196	M	74	Adenocarcinoma of the sigmoid with metastasis in the liver and lungs.
1180	M	78	Pulmonary hemorrhage, carcinoma of lungs, coronary heart disease.
1176	M	80	Arterio-sclerotic cardio-vascular disease.
1071	M	80	Arteriosclerotic cardio-vascular disease, anemia, hypertension.
1011	M	86	Coronary thrombosis.
1150	M	94	Broncho-pneumonia, pulmonary edema, duodenal ulcer.

2.3.1 Preparing, Mounting, and Storing Excised Bones

Upon excision, all bones were cleaned of flesh, placed in lidded jars containing 10% formalin solution, and stored thus at room temperature until bone mineral measurements could be made.

As time permitted, each bone was mounted on a separate $2\frac{1}{2}$" square of 1/8" thick clear acrylic sheet. Capitates were held to their plates with elastic bands. All other bones were fastened by anodized aluminum screws at two points well clear of the proposed measurement site. Each type of bone was mounted in a standardized orientation as illustrated in figure 2.2.5. Identification information was inscribed into the plates using a sharp scribe.

The mounted bones were x-rayed to assist in choise of the measuring site in a region of predominantly trabecular bone. X-rays were performed at a four to six foot distance, using 100mA at 60-75 kVP for 1/15 of a second. Sites for SED measurement were selected by inspection of the X-rays for all bone specimens except the femora, and positioning measurements taken from the X-rays. BMC scan paths were then made to pass through the SED site. Measurements of the acrylic mounting plates in the X-ray images revealed no magnification, so positioning measurements were

taken as absolute.

Femoral BMC scan paths were selected by inspection at the time of measurement, and were chosen at the narrowest portion of the femoral neck. Femoral SED measurement sites were taken at the center of the BMC scan path. Typical SED measurement sites and BMC scan paths are indicated in figure 2.2.5.

2.3.2 Preparing Bone Slices

After bone mineral content and specific electron density measurements were completed, a 1cm wide slice was cut from all bones other than the capitates. The slice was centered on the scan path of the G.E. Bone Mineral Analyzer, and was cut using a band saw with a blade having 16 teeth to the inch. Care was taken to feed the bone slowly past the blade so as to damage trabecular structure as little as possible. A paper tag labeled in pencil was attached to each slice by a thin wire at the periphery of the trabecular region.

The interstices of the bone slices were uniformally filled with paraffin to permit removal of a standardized volume of trabecular bone, and to assist in estimating trabecular, cortical and total slice volumes. The bone slices were first defatted by soaking overnight in 95% alcohol, one-half day in 100% alchol, and one-half day in zylol. Defatted slices were soaked approximately one hour in molten paraffin in a 62°C oven at a negative pressure of one atmosphere. Upon cooling, all excess paraffin was scraped from the slice using a scalpel.

2.3.3 Preparing Punch Volumes of Trabecular Bone

A right circular cylinder of paraffin-impregnated trabecular bone was punched from each slice, centered at the estimated point of specific electron density measurement. A specially-built biopsy-like coring tool, was used as in figure 2.3.1. The tool was made from 0.25 inch inside diameter stainless steel tubing with a polyethylene plunger and handle.

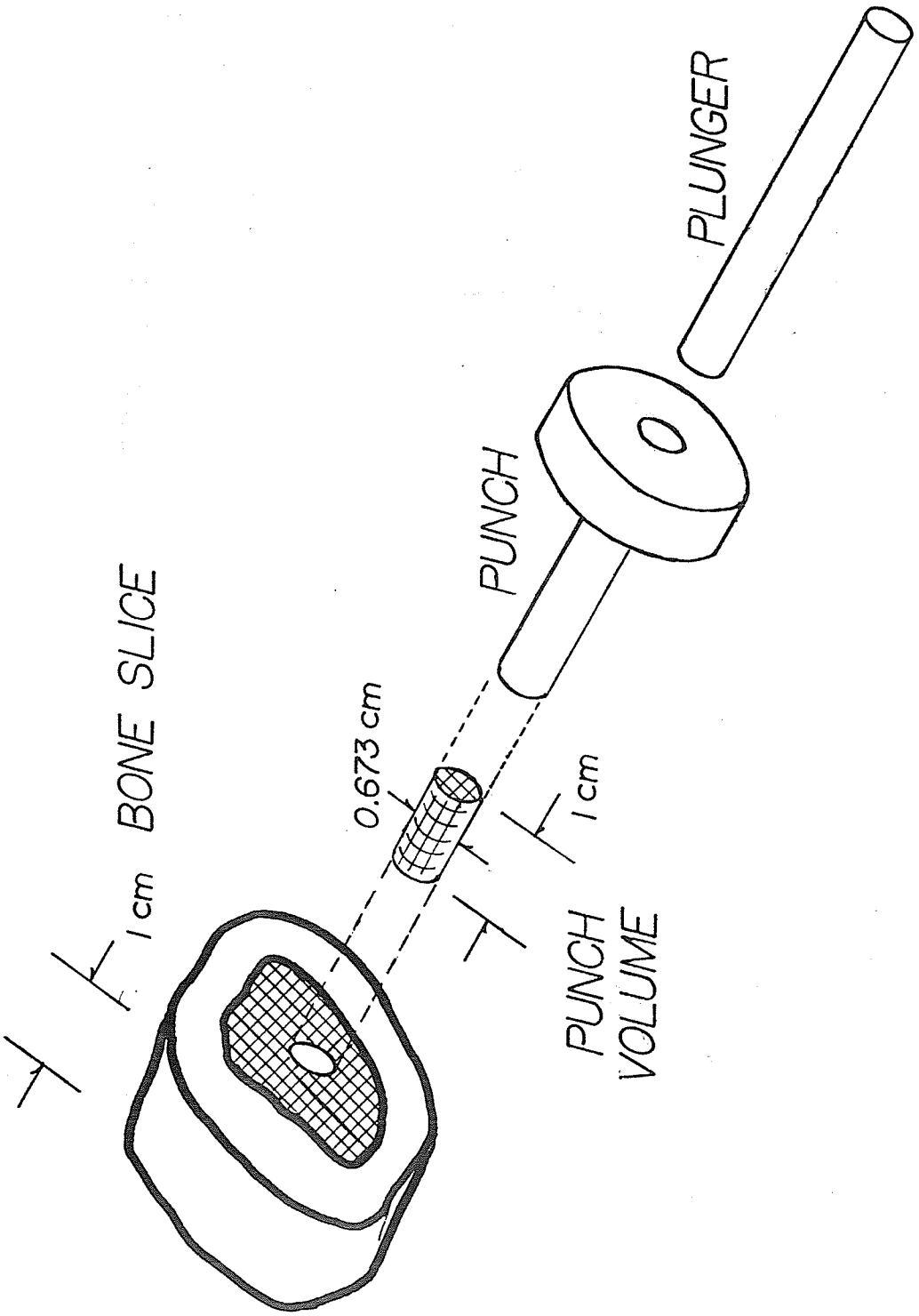

Figure 2.3.1 Apparatus for biopsying "punch" volumes.

2.3.4 Measuring Capitate, Bone Slices, and Punch Volumes

The volumes of the intact capitates and slices of the other excised bones were measured using a water displacement method, before the trabecular bone was punched from the center of the bone slices. First the weight of the dry bone or slice, together with an 80ml beaker filled to the brim with water, was measured on a one-pan triple-beam balance to the nearest 0.05g. The bone or slice was then totally immersed causing displaced water to overflow the rim of the beaker. A glass rod was touched to the rim so that surface tension would not prevent the displaced water from spilling over. The balance pan and the outside of the beaker were wiped dry, and the beaker, still containing the bone or slice, was reweighed. The weight of the water displaced was then calculated by subtracting the two weights taken. Bone slices were measured in this fashion at least twice, and capitates four times. The volume of each capitate and bone slice was then determined by dividing the mean weight of water displaced by the density of water at room temperature, which was taken to be 0.998g/ml. In retrospect, it is seen that the method was imprecise, with the standard deviation of the mean for an individual specimen being typically 2.5%, but on one occassion as high

as 7.8%.

The volume of the cylindrical core punched from the center of each bone slice was calculated from caliper measurements of core length and diameter. The length of each core was taken to be the mean bone slice thickness, which was measured to $\pm$0.01cm at four sites on the slice. The cross-sectional area of the core was calculated from the measured core diameter. The core diameter was found to be very uniform from one slice to the next, so the mean diameter of a random sample of 21 cores was taken as representative of all 60 cores. The mean core diameter was 0.637cm with a standard deviation of the mean of less than 0.1%.

2.3.5 Determining Ash Weight of Bone Specimens

After their volumes had been measured, the bone specimens were ashed, and the ashes weighed. The intact capitates were pre-dried for 24 hours at 60°C in a drying oven to prevent explosion due to formation of steam during ashing. Bone slices and trabecular punch volumes had already been dehydrated with ethanol as part of the paraffin impregnation procedure, and so were ashed directly. Each bone specimen was placed in a separate, numbered, nickel ashing crucible and heated in an ashing oven at 700 to 800°C for 24 hours.

After cooling, the bone ash specimens were weighed on an analytical balance. Each specimen was transferred to a tared polypropylene weighing planchet and net ash weight determined to the nearest decimal of a milligram. Nothing more was done with capitate and trabecular punch volume ashes.

Bone slice ashes were handled further to obtain separate cortical and trabecular ash weights. The trabecular portion of each bone slice specimen was removed from the cortical portion as completely as possible by scraping with a scalpel. The cortical ash was transferred to another tared planchet and weighed, a net slice cortical weight calculated. Total slice trabecular ash weight was calculated

by adding the trabecular punch volume ash weight to the difference between the original slice ash weight and the cortical ash weight. Total slice ash weight was taken as the original slice ash weight plus the trabecular punch volume ash weight. Finally, the percent of the slice ash weight due to trabecular bone was calculated.

Ash weights are summarized for each bone specimen type in table 2.3.1.

TABLE 2.3.1 Mean Ash Weights of Cadaver Bone Specimens.

Bone (N)	Mean Slice Ash Weight (Range)	Mean Cortical Ash Weight (Range)	Mean Trabecular Ash Weight (Range)	Mean Punch Ash Weight (Range)	Mean Percent Trabecular Bone of Ash Weight (Range)
Capitates* (20)	1.2886g (0.797-1.647g)	N/A	N/A	N/A	N/A
Radii (19)	1.2293g (0.6716-1.6087g)	0.4827g (0.2525-0.7460g)	0.7466g (0.3845-1.1360g)	0.0431g (0.0237-0.0620g)	60.3% (43% - 76%
Tibiae (10)	2.8260g (1.6961-3.6379g)	1.1873g (0.7215-1.7489g)	1.6387g (0.7954-2.2626g)	0.0421g (0.0129-0.0725g)	57.6% (47% - 69%)
Femora (9)	2.6082g (1.9714-3.6145g)	1.5366g (0.8205-2.4739g)	1.0715g (0.7334-1.5357g)	0.0250g (0.0174-0.0289g)	41.7% (32% - 58%)
Vertebrae (18)	1.0551 (0.7033-1.6517g)	0.5123 (0.2657-1.1904g)	0.5428 (0.3773-0.7836g)	0.0373 (0.0074-0.0635g)	52.7% (34% - 72%)

*Capitate values are for intact bone.

CHAPTER THREE

Accuracy, Precision and Sensitivity of the A.E.C.L. Bone Densitometer in Measuring Specific Electron Density Under Standardized Conditions

Before the in vitro and clinical studies were undertaken, a number of experiments were performed to assess the AECL Bone Densitometer's accuracy and precision in measuring specific electron density (S.E.D.). It was found that for homogeneous substances in standardized geometry, measured S.E.D. values correlated well with theoretical S.E.D. values ($r = 0.996$, $N = 12$). The specific electron density measured at a region within a homogeneous substance was found to vary with the size and shape of sample cross section by about 2.8% for lucite (SED = 1.16) and about 8.2% for aluminum (SED = 2.35). The sensitive volume was found to be diamond-shaped in cross-section, with effective diagonal dimensions of 4cm and 1.6cm, and with the long diagonal oriented vertically. Investigation of the dependence of S.E.D. readings upon surrounding material was not entirely conclusive, but it was demonstrated that the S.E.D. of lucite in an aluminum environment could be accurately measured under certain favourable circumstances. Reproducibility measurements on lucite and aluminum phantoms had coefficients of variation on the order

of 1% to 3%. A number of factors, including random and systematic sources of error, were identified which cast doubt on the AECL Bone Densitometer's usefulness for monitoring bone mineral status in humans.

3.1 The Relationship Between Measured and Calculated Electron Densities of Homogeneous Substances With Known Composition.

The specific electron densities (S.E.D.) of five substances of known composition, including water, were measured on the AECL Bone Densitometer and compared to calculated values based on chemical formulae. Measured S.E.D. values correlated well with calculated values ($r = 0.997$, $N = 4$), paralleled similar experimental results obtained by AECL-Commercial Products Division personnel ($r = 0.999$, $N = 8$). Figure 3.1.1 is a plot of the data, which appears in table 3.1.1.

Specific electron density (S.E.D.) was calculated as follows. Electron density (ED) of a substance is defined here as being the number of electrons per cubic centimeter of the substance. For an element, the electron density E.D.e is calculated from the formula

$$E.D.e = D\ No\ \frac{Z}{A} \quad . . . . . \quad 3.1.1$$

where D refers to physical density in grams per cubic cen-

timeter, No is Avogadro's number, and Z and A are the elements atomic number and mass number respectively (Garnett-1973). For a compound, the formula becomes

$$E.D._c = D\ No\frac{\left[\sum Ni\ Zi\right]}{\left[\sum Ni\ Ai\right]} \quad \ldots\ldots\ldots\ldots 3.1.2$$

where Ni refers to the number of atoms per molecule. Specific electron density of a substance is defined as the ratio of its electron density to that of water.

$$S.E.D. = \frac{E.D.\ substance}{E.D.\ water} \quad \ldots\ldots\ldots\ldots 3.1.3$$

Personnel at A.E.C.L.-Commercial Products Division in Ottawa measured prior to its shipment to Winnipeg. Cylindrical vials containing approximately 25ml. of water, sulfuric acid, xylene, hydrochloric acid, acetone, and benzene were measured, axis vertical, while inserted in a hole in a lucite block. Three vials containing aqueous solutions of potassium hydrogen phosphate in concentrations of 0.226g/ml, 0.447g/ml, and 1.016g/ml were likewise measured. Table 3.1.1 (a) lists the S.E.D. values obtained for all of these substances, along with the chemical formula, physical density and calculated S.E.D. figures. The correlation coefficient between calculated and measured specific electron density for this data is 0.999 (N=8).

The specific electron densities of four other substances were measured in this study, after the modifications described in 2.1.2 had been made. Solutions of pure chloro-

form and seventy percent (volume to volume) ethanol were measured contained in four-fluid ounce Dixie cups with no surrounding medium. Solid cylinders of lucite and aluminum, phantoms 1 and 5 respectively, were measured, centered at the beam intersection point, with long axis along each of the three orthogonal directions. A Dixie cup filled with water served as the standard. Table 3.1.1 (b) lists the chemical formula, physical density, and the calculated S.E.D. and measured S.E.D. values for these substances. S.E.D. values for the chloroform and ethanol solutions are based on single determinations, but values for phantoms 1 and 5 are mean values of 30 trials in each of the three orientations. The physical densities listed for acrylic and aluminum values obtained by weighing the two phantoms on an analytical balance, and measuring their dimensions with calipers. The correlation coefficient between calculated and measured specific electron density for this data os 0.997 (N=4). Figure 3.1.1 is a plot of the calculated versus the measured specific electron densities for the data in table 3.1.1.

TABLE 3.1.1 Calculated Specific Electron Densities (SED) for Various Substances.

(a) Measured by personnel of Atomic Energy of Canada, Ltd., Ottawa.

SUBSTANCE	CHEMICAL FORMULA	PHYSICAL DENSITY (g/cm^3)	CALCULATED S.E.D.	MEASURED S.E.D.
Acetone	CH_3COCH_3	0.79	0.79	0.79
Xylene	$C_6H_4\ (CH_3)_2$	0.87	0.85	0.83
Benzene	C_6H_6	0.88	0.86	0.82
Water	H_2O	1.00	1.00	1.00
Hydrochloric Acid	H CL	1.18	1.13	1.20
Potassium Hydrogen Phosphate	K_2HPO_4 (101.6%w/v)	1.17	1.15	1.15
	(44.68%w/v)	1.32	1.27	1.30
	(22.60%w/v)	1.67	1.55	1.59
Sulfuric Acid	H_2SO_4	1.84	1.70	1.85

(b) Present study measurements.

SUBSTANCE	CHEMICAL FORMULA	PHYSICAL DENSITY (g/cm^3)	CALCULATED S.E.D.	MEASURED S.E.D.
Ethanol	C_2H_5OH	0.85	0.86	0.87
Water	H_2O	1.00	1.00	1.00
Acrylic	$CH_2=C=CH_3-COOCH_3$	1.21	1.16	1.14
Chloroform	$CH\ CL_3$	1.48	1.27	1.43
Aluminum	Al	2.74	2.35	2.60

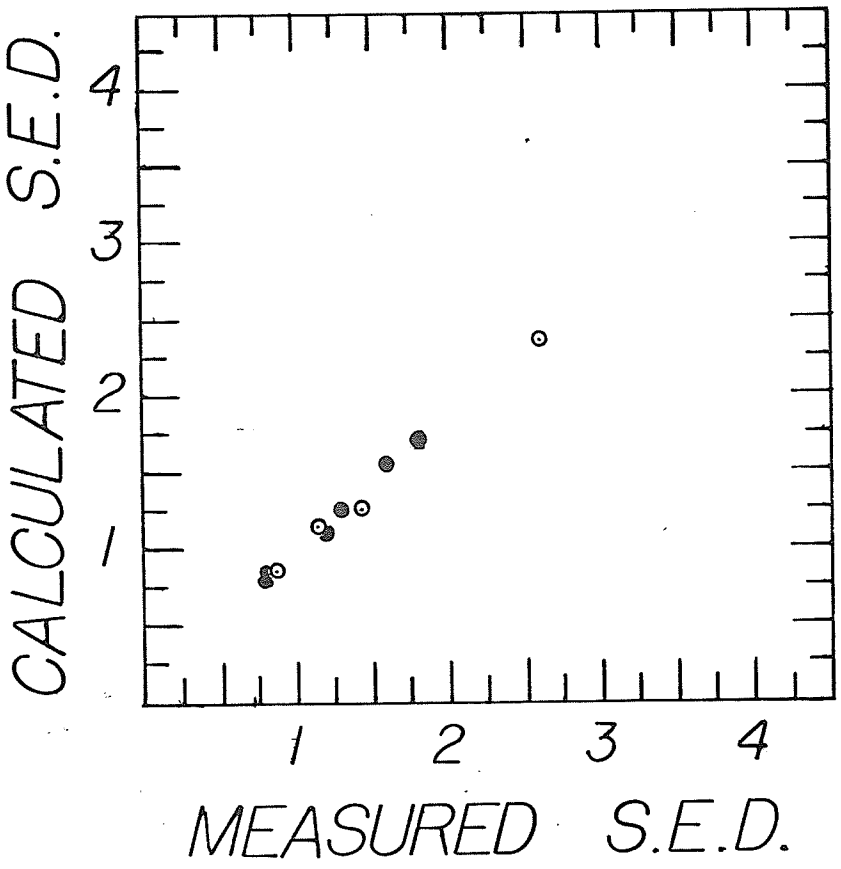

Figure 3.1.1 Calculated versus measured specific electron density (S.E.D.) closed circles are for Atomic Energy of Canada measurements and open circles are for this study.

3.2 The Relationship Between Specific Electron Density and Bone Mineral Content Measurements on a Femoral Head During Demineralization with Nitric Acid.

To determine the sensitivity of specific electron density (SED) measurements in monitoring changes in trabecular bone density, the SED of a femoral head was measured during demineralization with 4% nitric acid, and compared with parallel bone mineral content (BMC) readings in g/cm. One half of the head was sawed from the femur of one of the cadavers and screwed through the cortex to a $2\frac{1}{2}$" x $2\frac{1}{2}$" acrylic sheet. The mounted bone was placed in the lucite tank filled with water and measured on the AECL Bone Densitometer and the Bone Mineral Analyzer. The S.E.D. measurement site was found by inspection and the B.M.C. scan path chosen to pass through it. The bone was submerged in 4% (V/V) nitric acid, 10 volumes of acid per volume of bone, and stirred continuously with a magnetic stirrer. The bone was removed at 3 hours, 15 hours, and 23 hours for remeasurement on both instruments, and the nitric acid changed each time before replacing the bone. Only three pairs of SED, BMC measurements were obtained since the bone was so demineralized by 23 hours that the Bone Mineral Analyzer could not "see" the bone.

Despite the minimal data, there was reasonably good correlation between SED and BMC values ($r = 0.949$) and slightly better correlation between SED and BMC/BW values

(r=0.974). The lines of regression in the two instances are

$$SED = 0.0377\ BMC + 1.022 \quad . \quad . \quad . \quad . \quad . \quad . \quad . \quad . \quad . \quad 3.2.1$$

$$SED = 0.2614\ BMC/BW + 0.0984 \quad . \quad . \quad . \quad . \quad . \quad . \quad . \quad 3.2.2$$

From the slopes of the two regression lines, it can be estimated that a 5% change in BMC or BMC/BW would result in a 0.4 to a 0.6% change in SED. Thus it is readily apparent that although the AECL Bone Densitometer monitors specific electron density, and although SED may be determined to 1%, SED is an order of magnitued less sensitive in monitoring trabecular bone density changes than BMC or BMC/BW.

3.3 Verification of the Dimensions of the Volume Involved in Specific Electron Density Measurements.

Knowledge of the size and shape of the volume whose specific electron density (SED) is being measured is of considerable importance in the application of the A.E.C.L. Bone Densitometer to the problem of trabecular bone density monitoring. The volume must be sufficiently large to be representative of the average trabecular bone density in question, but must be small enough so as to include only trabecular bone, given the uncertainties in positioning likely to be involved. From the theoretical physics point of view, the smaller the sampling volume is, the less will be the error due to penumbral effects and multiple scattering. On the practical side, the smaller the volume, the lower will be the scattered conutrates observed, which would necessitate longer counting times. Therefore, the dimensions of the effective volume of beam intersection for the original 5mm diameter collimator apertures were investigated from several points of view.

First, measurements of collimator umbral and penumbral limits were taken from copies of the machinists drawings. The cross-section at the beam intersection point was diamond-shaped. For the source collimators, the dimensions

of the long and short diagonals of the umbral limits were 1.307cm and 0.541cm respectively, and those for the penumbral limits were 5.96cm and 0.91cm. The volumes calculated by consideration of the diamonds rotated about the long diagonal were $0.150cm^3$ and $1.94cm^3$ for the umbral and penumbral limits respectively. The formula used to calculate the sensitive volume (V_s) is

$$V_s = 0.393 \times \text{long diagonal} \times (\text{short diagonal})^2 \quad \text{. . eq. 3.3.1}$$

Similar measurements and calculations based on the detector collimator geometry indicate that the values of the penumbral diagonals are 5.25cm and 0.83cm resulting in a penumbral volume of $1.42cm^3$. The umbral values for the detector collimator are of course the same as for the source collimator.

Secondly, the beam intersection was visualized radiographically. Six dental films were taped together and positioned at the point of beam intersection, and exposed for one minute with the source at each of its two measurement positions. The films were developed using local dental film technique. An X-shaped image, with rather indefinite edges, resulted in five of the films, and the widths of the beam images varied according to the film's lateral position during exposure. The widest beam widths were approximately 0.8cm across, yielding an estimated sensitive volume of $0.62cm^3$. The formula relating sensitive volume

(V_s) to beam width (W) is

$$V_s = 1.202W^3 \quad \text{eq. 3.3.2}$$

The diagonal dimensions of the diamond-shaped intersection region were also measured from this film, and were estimated to be 2.1cm and 0.9cm and the volume of beam intersection was calculated to be 0.64cm by eq. 3.3.1. Thus some widening of the beam is evident, and the dimensions of the sensitive volume appear to fall between the two theoretical extremes calculated above. However, further studies indicated that the dimensions involved in a practical situation might be much larger.

In a third approach, the effective long diagonal was estimated by measuring the S.E.D. of a water standard as the stage was incrementally lowered. The S.E.D. value would be expected to decrease suddenly as the water level was lowered beneath the tip of the sensitive volume. This effect was observed to occur when the water level was about 2.06cm above the convergence point of the three positioning pointers. This would mean an effective long diagonal of approximately 4.13cm, an effective beam width of 1.58cm and a sensitive volume of $4.75cm^3$.

Also the effective beam width was estimated by moving a lead strip through the transmitted beam, and noting the points on either side of the beam at which penumbral ef-

fects caused a change in S.E.D. value. The lead strip was 1mm thick by 3mm wide by 9 mm long, and was taped to a $2\frac{1}{2}$ inch diameter lucite cylinder. The cylinder was oriented horizontally, centered at the sensitive volume, and rotated about its long axis in increments of approximately 0.05 radious. Also the edge of the lead strip encroached on the penumbral limits of the detector collimator's field of view, the measured S.E.D. value began to deviate from the value for the unobstructed beam. In this way the width of the penumbral limits of the detector collimator at $2\frac{1}{2}$ inches from the centre of the sensitive volume was determined to be a minimum of 1.58cm. Thus, the sensitive is estimated to be $4.74cm^3$.

From the foregoing evidence, it appears that the effective size of the sensitive volume is a function of the amount of material surrounding the intersection point of the photon beams. With a minimum of material at the beam intersection point, the sensitive volume is about $0.6cm^3$, and with a modicum of material present it is about $4.7cm^3$. This implies that the measured S.E.D. value would not be independent of the geometry of the object being measured and may account for some of the effects observed in section 3.4.

Perhaps even more important from the practical standpoint is the shape of sensitive volume and the change

in its dimensions with the amount of material present. In cross-section, the sensitive volume is diamond-shaped, with long diagonal oriented vertically. The length of the long diagonal is probably about 4cm which is larger than the dimensions of most deposits of trabecular bone measured in this study. The obvious consequence is that the cortical bone surrounding the trabecular bone of interest was unavoidably measured to some extent, and likely to a different extent, for each bone specimen and patient measured in this study. A related problem would occur if the tip of the diamond extended beyond the sample into air. To avoid this eventuality, all bone specimens were measured under a standard depth of water, and patients were measured with tissue-equivalent material surrounding their limbs.

3.4 The Effect of Surrounding Material on the Specific Electron Density Measurements at a Point.

The type, amount, and geometry of material surrounding the point of specific electron density (SED) measurement clearly affected the S.E.D. results, but the experiments performed were not definitive, and interpretation of the results is complicated by the presence of concurrent penumbral and beam inhomogeneity effects. Three types of experiments demonstrated the effects of surrounding media, but in each case the magnitude of the effect was modified by changes in beam collimation and beam homogeneity. One type of experiment investigated the effect of a small, dense piece of absorbing/scattering material; another type looked at the effect of various thicknesses and configurations of homogeneous material of low and high density; and the third studied the effect of a high density medium symmetrically surrounding a low density medium.

3.4.1 The Effect on Specific Electron Density Measurements of a Localized Region of Dense Matter Outside of the Measurement Region.

An experiment was performed to determine the effect on specific electron density (S.E.D.) measurements of a localized region of dense matter outside the S.E.D. measurement region. A 3mm wide by 1mm thick by 9mm long lead strip

was taped lengthwise to a $2\frac{1}{2}$ inch diameter lucite cylinder. The cylinder was oriented horizontally with its long axis perpendicular to the plane of the photon beams and rotated in increments of about 0.5 radious. S.E.D. measurements were made at each increment using the lucite cylinder as its own standard. Special multiaperture collimator inserts were placed successively in one source collimator, one detector collimator, and both the source and detector collimators on the same side of the instrument. Each collimator insert was a bundle of six small brass tubes which just fit into the existing collimator apertures. As the lead strip passed through each beam in twin, marked anomolies in S.E.D. measurements occured which were not greatly improved by better the collimation. Whereas some beam narrowing was observed, S.E.D. measurements were still 150% to 225% high at points where the lead strip was centered in one of the beam paths. Further, any beneficial effects due to such improved collimation would have been undermined by the drastic decrease in observed countrates, which would have meant impractically long measurement times. The experiment was a rather severe test of the Bone Densitometer's independence of sample geometry and chemical composition in that such highly dense material would not normally be encountered in measurements on bone. Nevertheless, the results indicate that a severely asymmetric arrangement of cortical bone, such as from a frac-

ture, might seriously affect the S.E.D. measurement.

3.4.2 The Effect on Specific Electron Density Measurements due to Varying Accounts of Homogeneous Material Surrounding the Sensitive Volume.

The measured specific electron densities of cylindrical lucite and aluminum phantoms were observed to vary with the orientation of the phantom, the effect being more severe for the aluminum phantom. Improved source and detector collimation as well as an artifactually introduced non-homogeneity in the transmitted beam increased the magnitude of the effect for both phantoms. Under instrument conditions as they prevailed during the present cadaver and clinical studies, the maximum difference in S.E.D. (maximum to minimum ratio) due to orientation was about 3.6% for the lucite phantom and 8.1% for the aluminum phantom.

Figure 3.4.1 (a) and (b) shows the cylindrical aluminum and lucite phantoms, and table 3.4.1 contains their measured S.E.D. values for the three orthogonal orientations, as obtained under various measurement conditions. Original measurements with the instrument as it arrived in Winnipeg shows maximum difference due to orientation of 9.6% and 25.5% for the lucite and aluminum phantoms, respectively. A bent attenuator may have been the cause, because replacement with locally-made lead attenuators improved the two results to

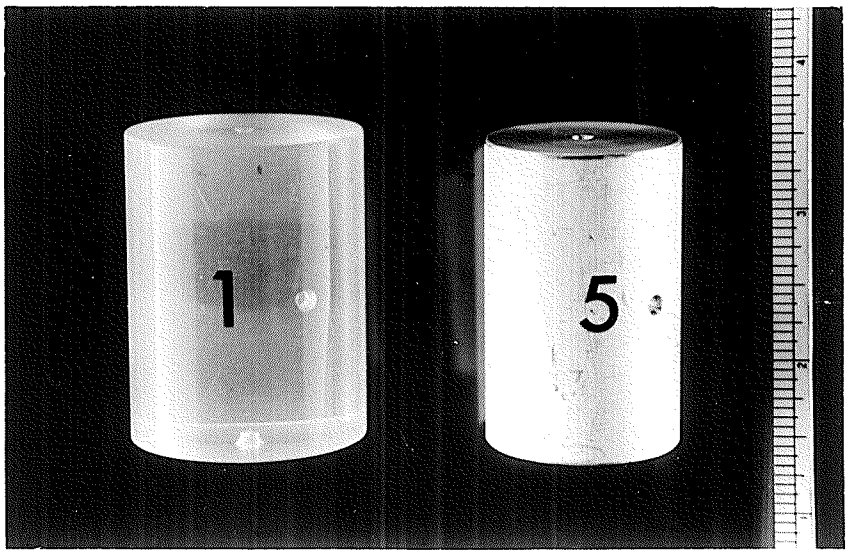

Figure 3.4.1 Cylindrical phantom.
(a) #5 - Aluminum ($1\frac{1}{4}$ inch diameter by 2 inch length).
(b) #1 - Lucite ($1\frac{1}{2}$ inch diameter by 2 inch length).

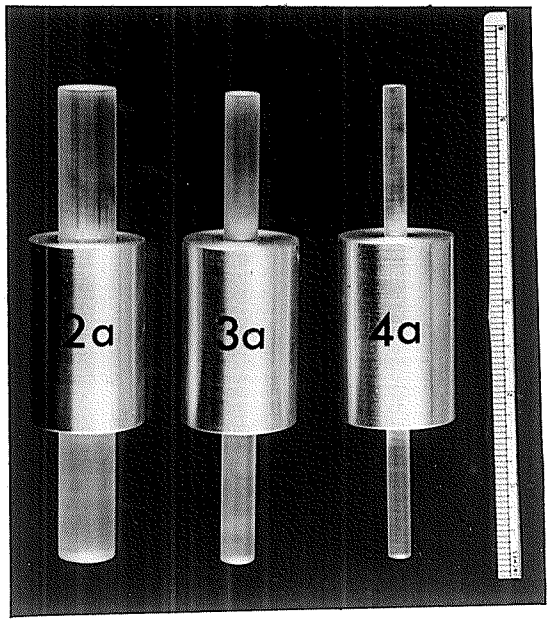

Figure 3.4.1-C Annular aluminum phantoms with lucite cores of diameters 5/8 inch, and 3/8 inch for phantom numbers 2a, 3a, and 4a respectively.

3.6% and 14.0%, respectively. Further improvement was achieved by using tin attenuators, which did not produce fluorescence radiation in the energy range selected by the scintillation detector discriminators. A third type of attenuator made by laminating strips of lead, tin, and copper to provide differential absorption of the lead fluorescence radiation, actually resulted in the least orientation effect, with maximum differences of 1.8% and 4.0%. Unfortunately, this was not noted at the time, and the tin attenuators, with orientation differences of 2.7% and 8.2%, were chosen on the basis of a comparison of the transmitted spectra for the three types of attenuator.

Figure 3.4.2 shows the scattered and transmitted spectra for each attenuator, and the tin attenuators definitely produce the most homogeneous photopeak for the transmitted beam. The scattered beam spectra are included to illustrate the necessity of removing the lead fluorescence radiation, which would be included in an energy window with a baseline low enough to include the entire scattered beam photopeak. Raising the baseline would reduce the already low scattered beam countrates even further, and increase the variability of countrate due to system gain or discriminator instability. The fraction of the lead fluorescence present in the transmitted beam spectrum would be expected to vary with the energy of the emergent transmitted beam in-

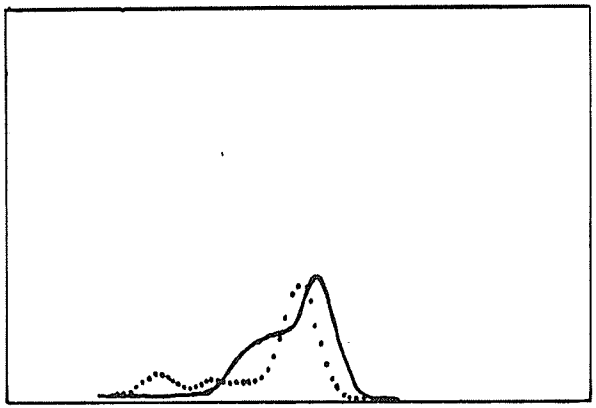

Pb ATTENUATORS

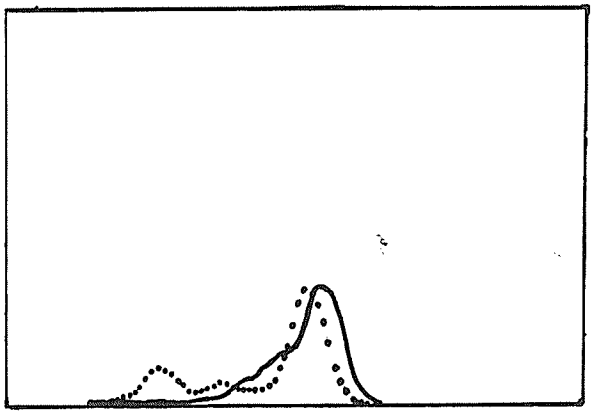

Pb/Sn/Cu/ATTENUATORS

Figure 3.4.2 Scattered (dotted) and transmitted (solid) beam spectra with various attenuator materials for the A.E.C.L. Bone Densitometer.

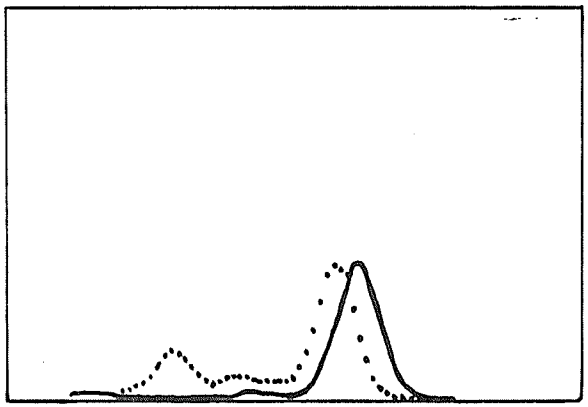

Sn ATTENUATORS

cident on the attenuator, which would be expected to undergo different degrees of "hardening" in traversing the aluminu, phantom as opposed to the water standard. Thus for high density materials, the transmitted beam countrate might be marginally less than it would be for a low density material due to proportionally less lead fluorescence. This would result in an artificially increased S.E.D. result, as observed.

3.4.3 Specific Electron Density Measurements of Cylindrical Lucite Phantoms Surrounded by Aluminum Annuli.

A set of three cylindrical lucite phantoms of varying diameter, surrounded by an aluminum annulus with outer diameter of $1\frac{1}{4}$ inches, shown in figure 3.4.1-c, were measured on the AECL Bone Densitometer in the three orthogonal orientations, with and without the brass collimator inserts shown in figure 3.4.3, and using various materials to attenuate the transmitted beam. The results indicate that under favorable conditions, the S.E.D. of a low-density core can be measured accurately even in the midst of a high-density environment.

Table 3.4.2 is a summary of S.E.D. values obtained. The phantom simulated a long bone in cross-section, and the object was to measure the specific electron density of the lucite with various amounts of aluminum surrounding it. In general, vertical orientation gave better results than hori-

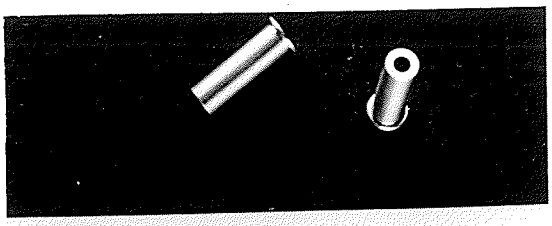

DETECTOR INSERTS
length: 5/8"

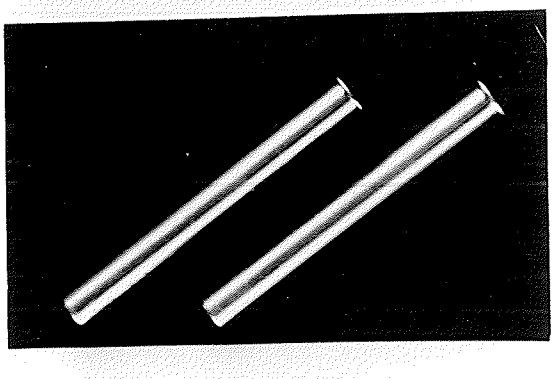

SOURCE INSERTS
length: 2 1/16"

Figure 3.4.3 Brass collimator inserts for A.E.C.L. Bone Densitometer.

TABLE 3.4.1 Effects on Measured Specific Electron Density Measurements due to Phantom Orientation.

	SPECIFIC ELECTRON DENSITY					
	LUCITE PHANTOM (#1)			ALUMINUM PHANTOM (#5)		
	Vertical	Horizontal X-Axis	Horizontal Y-Axis	Vertical	Horizontal X-Axis	Horizontal Y-Axis
Original Attenuators No Collimator Inserts	0.83 (1) [9.6%]	0.91 (1)	0.87 (1)	2.46 (1) [25.5%]	2.08 (1)	1.96 (1)
Lead Attenuators No Collimator Inserts	1.16 (20) [3.6%]	1.13 (20)	1.12 (20)	3.07 (20) [14.0%]	2.71 (20)	2.71 (20)
Lead/Tin/Copper Attenuators No Collimator Inserts	1.16 (20) [1.75%]	1.13 (20)	1.14 (20)	2.63 (20) [4.0%]	2.53 (20)	2.54 (20)
Tin Attenuators No Collimator Inserts	1.15 (22) [2.8%]	1.13 (22)	1.12 (20)	2.78 (22) [8.2%]	2.57 (20)	2.57 (20)
Tin Attenuators Brass Collimator Inserts	1.16 (1) [3.6%]	1.14 (1)	1.13 (1)	2.76 (1) [11.7%]	2.47 (1)	2.47 (1)

S.E.D. values are mean of 1 to 22 measurements over 1 to 25 days. Numbers in round brackets are the number of measurements used in calculating the mean.

The percentages in the square brackets in the "vertical" columns are maximum percent differences due to other orientations, relative to the vertical value.

zontal orientation, but the results for horizontal orientation were undoubtedly artificially high due to the sensitive volume dimensions being larger than the lucite core dimensions, especially when no collimator inserts were used. The brass collimator inserts definitely improved the accuracy by decreasing the size of the sensitive volume. Both the lead/tin/copper and the tin attenuators gave better results than the lead attenuators. Only with the combination of lead/tin/copper attenuators plus the brass collimator inserts was an accurate S.E.D. value, (SED = 1.17), for the lucite core obtained in both vertical and horizontal orientations.

TABLE 3.4.2 Summary of specific electron densities obtained on a set of three annular aluminum phantoms with cylindrical lucite cores measured in the three otthogonal directions under various circumstances.

S.E.D. Measurement Conditions	M E A S U R E M E N T								
	# 2 a			# 3 a			# 4 a		
	Vertical	Horizontal (X-Axis)	Horizontal (Y-Axis)	Vertical	Horizontal (X-Axis)	Horizontal (Y-Axis)	Vertical	Horizontal (X-Axis)	Horizontal (Y-Axis)
Pb Attenuators, In air, No brass collimator inserts			1.48 (20)						
Pb/Sn/Cn Attenuators, In air, No brass collimator inserts	1.17 (1)	1.44 (1)	1.44 (20)	1.28 (1)	1.82 (1)	1.77 (1)	1.62 (1)	2.05 (1)	2.12 (20)
Sn Attenuators, In air, No brass collimator inserts	1.29 (1)	1.48 (1)	1.40 (1)	1.41 (1)	1.78 (1)	1.79 (1)	1.79 (1)	2.16 (1)	2.09 (1)
Pb Attenuators In air, With brass collimator inserts			1.26 (20)						1.90 (20)
Pb/Sn/Cu Attenuators In air, With brass collimator inserts			1.17 (21)						1.51 (21)

Numbers in brackets are the number of measurements in the set.

S.E.D. values are means where more than measurement was taken.

3.5 Reproducibility of Specific Electron Density Measurements of a Lucite and an Aluminum Phantom.

The specific electron density (S.E.D.) of cylindrical phantoms of lucite and aluminum were measured many times over a 26 month period for quality assurance pruposes, and found to have coefficients of variation 1.0 to 3.2% and 2.1 to 2.7%, respectively, under various conditions. The phantoms are pictured in figure 3.4.1, (a) and (b), and a summary of the results appears in table 3.5.1.

An early study was done in February and March, 1973, to compare accuracy and reproducibility of S.E.D. measurements using two different attenuator materials. Twenty S.E.D. measurements over a three week period were made on both the lucite and aluminum phantoms in vertical orientation using the lead attenuators, and a similar set of twenty measurements were made with the lead/tin/copper attenuators over a subsequent four day period. The lead/tin/copper attenuators produced more accurate results for the aluminum phantom (SED = 2.63) than did the lead attenuators (SED - 3.09), but the variances for the two types of attenuator were not significantly different ($F = 1.23$ for 19,19df). For the lucite phantom, the mean S.E.D. was 1.16 and the coefficient of variation was 1.4% for both attenuator types.

Another study, performed in November 1973, after repair of the Bone Densitometer, following a fault, and using

tin attenuators, produced essentially the same results as the earlier study for the lucite phantom (SED = 1.15, %C.V. = 1.4%). The mean S.E.D. value for the aluminum phantom, however, was slightly higher (SED = 2.78) than it had been for the lead/tin/copper attenuators, but was slightly better than it had been for the lead attenuators. The variance of the aluminum phantom readings using the tin attenuators was not significantly different from the previous study.

TABLE 3.5.1 Quality assurance S.E.D. measurements on cylindrical lucite and aluminum phantoms.

			LUCITE: VERTICAL			ALUMINUM: VERTICAL		
	CONDITIONS	DATES	MEAN	%C.V.	N	MEAN	%C.V.	N
Source # 1	Pb Attenuators, No Collimator Inserts, Pre-failure	Feb. 7-Mar. 1/73	1.16	1.4%	20	3.09	2.7%	20
	Pb/Sn/Cu Attenuators, No Collimator Inserts, Pre-failure	Mar.20-22 1973	1.16	1.4%	20	2.63	2.1%	20
	Sn Attenuators No Collimator Inserts Post-repair	Nov.10-29	1.15	1.4%	22	2.78	2.5%	22
	Sn Attenuators No Collimator Inserts:	Mar./74	1.13	3.2%	4			
	Clinical studies	Apr./74	1.16	1.0%	8			
		May /74	1.15	2.6%	9			
Source # 2	Sn Attenuators No Collimator Inserts:	Nov,/74	1.17	1.7%	18			
	Bone specimens and clinical studies	Dec./74	1.17	2.3%	18			
		Jan./75	1.17	2.2%	19			
		Feb./75	1.17	1.5%	6			
		Mar./75	1.16	1.3%	10			
		Apr./75	1.16	2.6%	8			

From March 1974 to the end of the study in April 1975, the lucite phantom is verticle orientation was measured in conjunction with each set of bone specimen, or clinical, S.E.D. measurements. Mean S.E.D. values and coefficients of variation were calculated for each month and are also listed in table 3.5.1. The relatively high C.V. values for March to May 1974 probably reflect the aging of the source, as well as the longer time span within each data set. After the new source arrived in November 1974, monthly mean S.E.D. values were slightly higher and quite stable at 1.16 or 1.17. A t-test shows that this increase, although small, is statistically significant ($p < 0.001$), but the reason for the difference is not known. Monthly coefficients of variation for the new source ranged from 1.3% to 2.6% over the last six months of the study, during which time all of the bone specimen measurements and the majority of the clinical measurements were made.

3.6 Error Considerations

A number of possible sources of error in specific electron density measurement with the A.E.C.L. Bone Densitometer may be postulated, although a detailed quantitative analysis of error is beyond the scope of this study. For the purpose of the present discussion these errors will be considered in the following categories: errors involving basic theoretical assumptions, errors peculiar to the A.E.C.L. Bone Densitometer, and errors in clinical applications.

Kennett-1976 investigates inhereat sources of error for a two photon Compton scattering method employing similar energies as the A.E.C.L. Bone Densitometer and based on the same theory. He identified systematic errors as due to finite beam geometry, non-identity of geometry for scattered and transmitted beams, and multiple scattering. Finite geometry refers to the fact that photon beam widths have finite dimensions in reality, whereas the theory is based on infinitesimal beam widths. With finite geometry, the atteunation facturs do not cancel completely due to unequal path lengths at extremes of the beam. By proposing a simple geometric model, Kennet calculates that an apparent increase in density of only about 1% may be expected with his system, and he concludes that finite geometry affects may be ignored. Since the present system uses collimator diameters (5mm) smaller than those in Kennett's system (8mm), it may be as-

sumed that errors due to finite geometry are also negligible for the A.E.C.L. Bone Densitometer. Non-identity of geometry for scattered and transmitted beams results because the dimension of the transmitted beam is determined solely by the detector collimator, while the shape of the scattered beam is determined by a combination of source and detector collimators. Again using a simple geometric model Kennett concludes that errors due to non-identical beam geometry cause increases in apparent density of about 1%, and so may be ignored. Therefore, such errors are probably also insignificant with the Bone Densitometer. In contrast to these two sources of error, Kennett found multiple scattering of photons before detection to produce increases in apparent density.

His analysis indicates that multiple of up to 10% scattering effects decrease as the fraction of photoelectric interactions increases, which would be a function of the Z/A ratio of the sample measured and also of the transmitted and scattered beam energies. Although Kennett proposes an apparently successful empirical correction based on the quality of the detected transmitted beam, no such corrections were made in the present study. All three of the systematic errors discussed here result in elevated values and so would be additive. Therefore, it is possible that A.E.C.L. Bone Densitometer measurements may have been up to 12% falsely

high. However, Kennett's analysis was based on 90° scattering angle and quantitative error estimates may not be applicable to the present situation.

Several factors peculiar to the A.E.C.L. Bone Densitometer design may also contribute to the overall error in specific electron density measurement. One such factor would be long-lived ^{152}Eu and ^{154}Eu impurities in the source, which would influence results increasingly as the primary ^{153}Gd decayed. Since these impurities emit a number of high energy photons, transmitted and scattered beams would not be affected in the same manner as for the low energy emissions of ^{153}Gd. Another factor would be spectral artifacts due to the interposition of attenuators in the path of the transmitted beam. Although some improvement was noted when tin attenuators were used instead of lead ones, other types of attenuator material might have improved results even more (section 3.5).

Electronic instability of discriminator levels and/or detector high voltage may have been an important cause in the lack of reproducibility of phantom readings over long periods of time. This would be a random error, and its magnitued was not estimated. On the other hand, the error due to the statistics of radioactive decay may be estimated. The Poisson Law was applied to the countrates in the equation for specific electron density (equation 2.1) and the expression for the

percent standard error in S.E.D., due to decay statistics only, was found to be

$$\% \text{ Standard error in S.E.D.} = 50\sqrt{\sum \frac{1}{Ri}} \qquad 3.6.1$$

where Ri refers to the eight countrates observed in any one S.E.D. measurement. Substituting typical countrate values indicates that errors due to the randomness of decay alone ranged between 1.7 and 2.3%. Finally, the A.E.C.L. Bone Densitometer had no provision for subtracting background countrates. Although background countrates were normally only about 70 counts per minute, the scattered countrates were only about 1000 counts per minute. Thus, even though counting times were increased to compensate for source decay, systematic errors due to ignoring background may have resulted in S.E.D. values that were 1.5% too high.

Three more sources of error are added when the A.E.C.L. Bone Densitometer is applied to the in vivo measurement of trabecular bone. First is the uncertainty in positioning the sensitive volume of Densitometer in the region of trabecular bone desired, when only surface anatomy landmarks are used. Second is the uncertainty of the effective dimensions of the sensitive volume, which apparently change with the amount of scattering, and which may have resulted in the inadvertant inclusion of some cortical bone (section 3.3). Third is the uncertainty in the proportion of fat in

the cancellous bone marrow. Since specific electron density is more sensitive to changes in fat content than to changes in trabeculation (section 4.4), this is a severe limitation to the use of the A.E.C.L. Bone Densitometer for measuring trabecular bone density.

CHAPTER FOUR

Relations Between Appendicular and Axial Skeleton Bone Mineral Status in Ten Cadavers.

If the A.E.C.L. Bone Densitometer is to be a useful clinical instrument for in vivo monitoring of skeletal bone mineral status two conditions must be met. The first is that the measurements of specific electron density (S.E.D.) made with the Densitometer must be an accurate measure of skeletal mineral status at the site measured. The second is that the bone mineralization at the site measured must reflect the mineralization of the skeleton in general, or that at skeletal sites of special clinical concern, such as the spine and the femoral neck. This chapter presents the results of a series of in vitro studies on excised cadaver bones which investigate these conditions individually.

A threefold approach was adapted, including gravimetric bone ash measurements, Bone Densitometer specific electron density measurements, and Bone Mineral Analyzer (BMA) measurements. The bone ash measurements served as the fundamental basis of assessing the Bone Densitometer's ability of monitoring trabecular bone mineral status. Bone Mineral Analyzer measurements were made at the same sites so a direct comparison could be made between Bone Densitometer re-

sults and those of a widely accepted standard method of bone mineral content assay.

In assessing the various correlations among combinations of the three modes of bone mineral measurement and skeletal sites, certain data were either not available or were excluded in particular comparisons as appropriate. One ninth vertebral and one femoral neck slice did not get ashed, and one eighth vertebra was not excised intact. One left radius was heavily calcified at the measurement site so the trabecular measurements could not be made. One femur, one eighth vertebra, and one ninth vertebra had heavily calcified cortices, and any measurements on these bones which included cortical bone in the measurement were excluded from computations of correlation coefficients involving biological comparisons between skeletal sites.

4.1 Relations between Bone Ash Measurements From Five Accessible and Three Inaccessible Skeletal Sites.

To investigate the relationship between bone mineral status at various skeletal sites, a bone ash study was performed. Eight bones were excised from each of ten cadavers, comprising left and right distal radii and capitates, one distal tibial, one proximal femur, and the eighth and ninth thoracid vertebrae. The radii, capitates and tibia were considered to be appendicular skeletal sites "access -

ible" to the AECL Bone Densitometer, and the femoral neck and vertebrae to be "inaccessible" but clinically important skeletal sites. Sections were cut from trabecular sites on the long bones and vertebrae and ashed along with the intact capitates. The ash weight of the trabecular portion of each bone section was obtained as well as the composite ash weight and ash density for the complete section. Only the composite ash weights were made, for both composite and trabecular ash measurements, between the five "accessible" skeletal sites and the three "inaccessible" skeletal sites.

4.1.1 The Relationships Between Ash Measurements of Composite Bone Specimens.

The ash weights and ash densities of composite bone specimens from six appendicular and two axial skeletal sites were measured, and some pertinent correlations investigated. Appendicular specimens were the intact left and right capitates along with 1cm slices taken from one femoral neck, one distal tibial metaphysis, and both distal radial metaphyses. One centimeter wide coronal sections from the eighth and ninth thoracic vertebrae comprised the axial specimens. The ash density of a bone slice specimen refers to the ash weight of the slice divided by the slice volume as determined before ashing. For correlation purposes, the capitates and the radial and tibial specimens were considered as representing

"accessible" skeletal sites, and the femoral neck and vertebral specimens as representing "inaccessible" skeletal sites. Associations between accessible and inaccessible sites were analysed for both ash weights and ash densities, and the correlation coefficients appear in table 4.1.1. No very strong relationships were found in either case, but the correlations for ash weights were slightly better on the average than those for ash densities. Figure 4.1.1 is a scattergram of intact capitate ash weights versus vertebral slice ash weights.

The bone ash weight (B.A.W.) of the capitates correlated well with the slice ash weight (S.A.W.) of the vertebrae. Coefficients ranged from $r = 0.59$ to $r = 0.97$, and three of the four were significant at the 5% level or better (Sokal-1973). The correlation between capitate B.A.W. and femoral neck S.A.W. was somewhat less marked, $r = 0.55$ and $r = 0.64$ for left and right capitate respectively, and a larger sample would have to be taken to determine whether a real relationship exists between these sites.

Somewhat similar results were obtained between S.A.W. of the radii and S.A.W. for the inaccessible sites. All four of the correlations between radii and vertebrae were significant at the 5% level or better. The coefficients obtained ranged from $r = 0.1$ (8) to $r = 0.85$ (8), and are comparable to those obtained by Wilson-1972 for BMC of the distal radius

against BMC of the eighth and ninth vertebrae ($r = 0.66$ to $r = 0.70$). However, the present study does not disclose the same high correlation ($r = 0.87$) between radius and femoral neck formed by Wilson. The reason for this discrepancy may lie in the fact that the size and shape of the femoral neck varies considerably in the region between the trochanter and the head, as well as from one individual to another. In the present study a single slice from the femoral neck was ashed, whereas Wilson made three sets of four or five scans to obtain an average femoral neck BMC value. Also Wilson measured a much more cortical radial site. The slice ash weight (S.A.W.) of the distal tibia correlated better with the S.A.W. of the vertebrae, $r = 0.69$ (8) and $r = 0.77$ (8), than with the S.A.W. of the femoral neck, $r = 0.49$ (8).

Correlations between ash densities are in general somewhat lower than those between corresponding ash weights. Capitate bone ash density (B.A.D.) correlated poorly, $r = 0.23$ and $r = 0.27$, with slice ash density (S.A.D.) of the femoral neck, but moderately well with S.A.D. of the vertebrae, $r = 0.73$ (8) to $r = 0.77$ (8). Radial S.A.D. compared weakly with femoral neck S.A.D., $r = 0.661$ and $r = 0.685$, and even less well with vertebral S.A.D., $r = 0.39$ (7) to $r = 0.66$ (8). Tibial ash density correlations were the weakest on the

whole, with a coefficient of r = 0.63 (8) with the femoral neck, and coefficients of r = 0.24 (8) and r = 0.42 (8) for the eighth vertebra and ninth vertebra, respectively. Only the correlation coefficients between capitate B.A.D. and vertebral S.A.D., were significant at the 5% level.

Although some of the inconsistency in the above relationships may be due to small sample size, the poorer nature of the findings for densities compared to weights agrees with that of a study reported by Horsman-1970, in which the weights and the weight/volume ratios of whole bones of 23 male skeletons were compared. He found that radial and second metacarapal weights correlated significantly, albeit only moderately well, with the weight of the spine, r = 0.59, 0.62 respectively, and similarly with the third lumbar vertebra, r = 0.70, 0.64 in the same order. In contrast, none of the weight/volume ratios of the appendicular bones correlated strongly with the weight/volume ratio of the spine: r = 0.09 for the radius and r = 0.43 for the second metacarpal. In comparing radial and metacarpal weights to femur weights the correlation coefficients were r = 0.92 and r = 0.88, respectively, whereas, the corresponding coefficients for weight/volume ratios were r = 0.56 and r = 0.79.

Thus, it would appear that the absolute weights of composite bone specimens correlate better than do their densities when comparing specimens from the accessible and the inaccessible skeletal sites.

TABLE 4.1.1 Correlation coefficients between composite bone ash measurements at accessible and inaccessible skeletal sites.

(a) Correlation Coefficients between Slice Ash Weights (S.A.W.).

	FEMOR NECK S.A.W.	8^{th} VERTEBRA S.A.W.	9^{th} VERTEBRA S.A.W.
LEFT CAPITATE* B.A.W.	0.55 (8)	0.93 (8)	0.73 (8)
RIGHT CAPITATE* B.A.W.	0.64 (8)	0.97 (9)	0.59 (8)
LEFT RADIUS S.A.W.	0.29 (7)	0.71 (8)	0.68 (8)
RIGHT RADIUS S.A.W.	0.53 (8)	0.85 (8)	0.61 (8)
TIBIA S.A.W.	0.49 (8)	0.69 (8)	0.77 (8)

(b) Correlation Coefficients between Slice Ash Densities (S.A.D.).

	FEMUR (S.A.D.)	8th VERTEBRA (S.A.D.)	9th VERTEBRA (S.A.D.)
LEFT CAPITATES* B.A.D.	0.22 (8)	0.73 (8)	0.338 (9)
RIGHT CAPITATE* B.A.D.	0.27 (8)	0.76 (8)	0.77 (8)
LEFT RADIUS S.A.D.	0.66 (7)	0.50 (7)	0.39 (7)
RIGHT RADIUS S.A.D.	0.69 (8)	0.66 (9)	0.53 (8)
TIBIA S.A.D.	0.63 (8)	0.24 (8)	0.42 (8)

*Capitate values are for total bone.

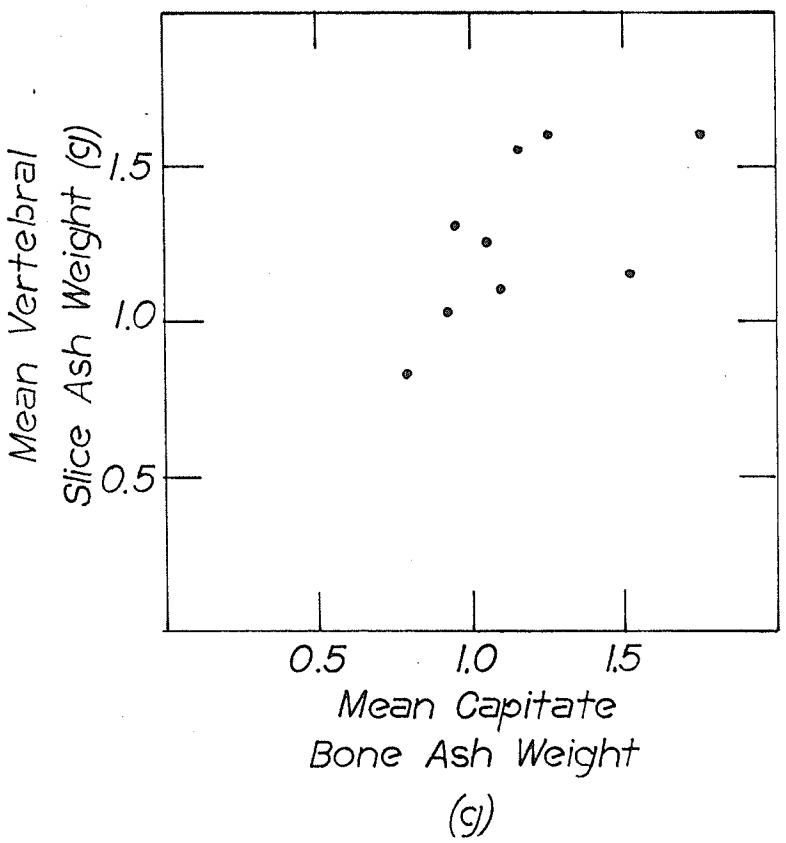

Figure 4.1.1 Scattergram between mean vertebral (8th and 9th thoracic) slice ash weight and mean capitate (left and right) bone ash weight.

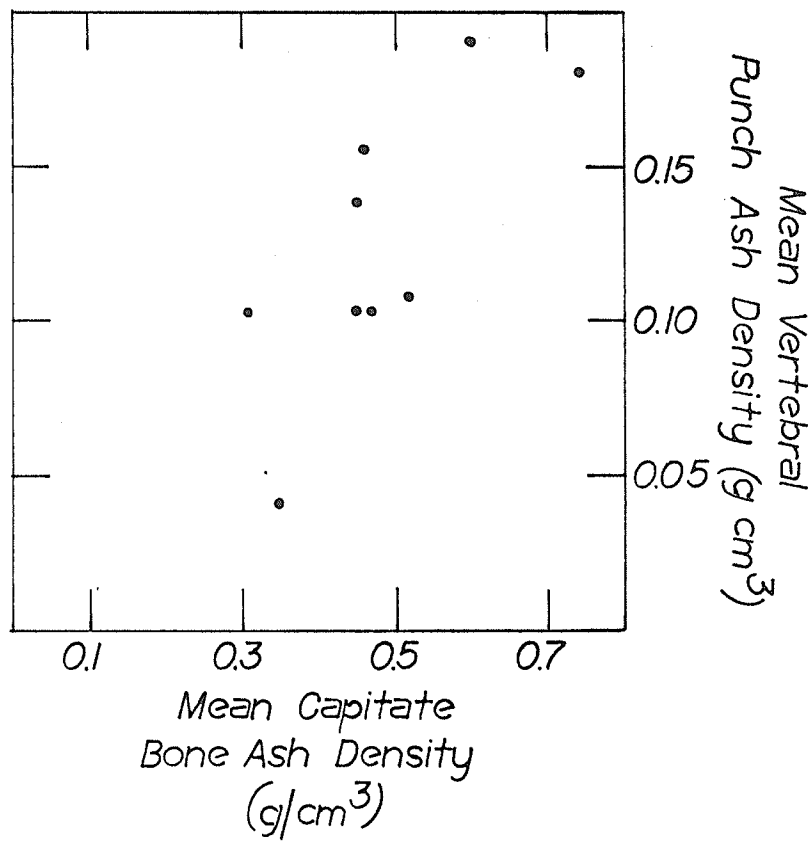

Figure 4.1.2 Scattergram between mean vertebral (8th and 9th thoracic) punch ash density and mean capitate (left and right) bone ash density.

4.1.2 The Relationships Between Trabecular Bone Ash Measurements.

The relationships between trabecular-bone ash measurements at the six appendicular and two axial skeletal sites were investigaged. The total ash weight of the trabecular structure scraped from the composite bone slices was compared between accessible and inaccessible skeletal sites. The capitates were included in these comparisons even though they were ashed whole. In addition, the "punch ash densities" of these sites were inter-compared. Punch ash density refers here to the ash weight of a $0.32cm^3$ volume "punched" out of the trabecular portion of each bone slice before ashing, as described in 2.3.3. Associations for ash weights between accessible and inaccessible sites ranged from moderate, but significant (r = about 0.7), to non-existant (r = less than 0.2). In general, corresponding relationships for punch ash density between these sites were less marked than for the corresponding relationships for trabecular ash weight, except for the capitate relationships, which are a special case. Table 4.1.2 contains the correlation coefficients between accessible and inaccessible sites for both weights and densities and figure 4.1.2 is a scattergram of intact capitate ash densities versus vertebral slice ash densities. The only relationship found for trabecular bone between an accessible site and an inaccessible site was capitate bone ash density (B.A.D.), versus vertebral punch ash density (P.A.D.), and this corre-

lation was only moderately strong r = 0.68 (9) to r = 0.78. These results cast some doubt on the advisability of making point measurements of trabecular bone density at accessible sites for the purpose of predicting trabecular bone density at inaccessible skeletal sites.

Correlations for trabecular ash weight (T.A.W.) between accessible sites and inaccessible sites were weak at best, and in general poorer than corresponding comparisons for slice ash weights. It is not certain whether any of the associations are meaningful since only two were significant at the 5% level, namely right capitate B.A.W. versus eighth vertebra T.A.W., and left capitate B.A.W. versus ninth vertabra T.A.W. The range of correlation coefficients between capitate B.A.W. and vertebral T.A.W. was r = 0.39 (9) to r = 0.67 (9), and that between radial T.A.W. and vertebral T.A.W. was r = 0.23 (9) to r = 0.59 (9). The association between accessible sites and femoral neck T.A.W. ranged from r = 0.40 (8) to r = 0.65 (8). The poorest associations were between T.A.W. of the tibia and the accessible sites, r = 0.06 (9) to r = 0.41 (9).

Punch ash density (P.A.D.) correlations between accessible sites and inaccessible sites are very poor, except the relationship between capitate bone ash density (B.A.D.) and vertebral P.A.D. Correlation coefficients between P.A.D.

TABLE 4.1.2 Correlation coefficients between trabecular bone ash measurements at accessible and inaccessible skeletal sites.

(a) Correlation Coefficients between Trabecular Ash Weights (T.A.W.)

	FEMORAL NECK T.A.W.	8th VERTEBRA T.A.W.	9th VERTEBRA T.A.W.
LEFT CAPITATE* B.A.W.	0.63 (8)	0.39 (9)	0.67 (9)
RIGHT CAPITATE* B.A.W.	0.58 (8)	0.67 (9)	0.58 (9)
LEFT RADIUS T.A.W.	0.52 (7)	0.35 (9)	0.57 (9)
RIGHT RADIUS T.A.W.	0.65 (8)	0.23 (9)	0.59 (9)
TIBIA T.A.W.	0.40 (8)	0.06 (9)	0.41 (9)

(b) Correlation Coefficients between Trabecular "Punch" Ash Densities (P.A.D.)

	FEMUR P.A.D.	8th VERTEBRA P.A.D.	9th VERTEBRA P.A.D.
LEFT CAPITATE* B.A.D.	0.59 (8)	0.78 (9)	0.73 (9)
RIGHT CAPITATE* B.A.D.	0.49 (8)	0.74 (9)	0.68 (9)
LEFT RADIUS P.A.D.	0.68 (7)	0.27 (9)	0.14 (9)
RIGHT RADIUS P.A.D.	0.29 (8)	0.44 (9)	0.32 (9)
TIBIA P.A.D.	0.59 (8)	-0.13 (9)	-0.10 (9)

*Capitate values are for total bone.

of the femoral neck and P.A.D. (or B.A.D.) of the five accessible sites ranged from r = 0.29 (8) to r = 0.68 (7), which is about the same as was obtained for the composite bone S.A.W. comparisons. Coefficients between P.A.D. of the vertebrae and P.A.D. of the tibia and radii ranged from r = -0.10 (9) to r = 0.44 (9). In contrast, capitate B.A.D. correlated significantly (5% level), although only moderately, r = 0.68 (9) to r = 0.78 (9), with P.A.D. of the vertebrae.

The ash measurement data of this study indicate that composite bone ash weights at accessible sites correlate better than corresponding trabecular ash weights. This result is in keeping with the conclusion arrived at by Dalen-1973, in an in vivo study of bone mineral content at various appendicular and axial sites of cortical and trabecular bone. Using a dual energy, x-ray spectrophotometric method (Jacobson-1964), he measured the bone mineral content of the distal and medial radius and ulna, head of the humerus, third lumbar vertebra, femoral neck and shaft, and calcaneus. He reports that "trabecular sites showed greater biological variation that did the cortical sites". Similarly, in data by Wilson-1972, BMC at medial sites of the radius, ulna, humerus, tibia, fibula, and femur of 24 embalmed skeletons showed less variation (mean %C.V. = 27.9%) than corresponding distal sites (mean %C.V. = 30.4%). In the present study no predominantly cortical bone

sites were studied, but the biological variation of the mixed-bone ash weights (mean %C.V. = 23.6%) was in fact less than those for the trabecular ash weights (mean %C.V. = 40.4%). It is not surprising then that correlations between the mixed-bone ash weights are stronger than those between the trabecular ash weights.

The poorer correlations observed in the present study between radial and tibial P.A.D. versus vertebral P.A.D., in comparison to corresponding correlations for trabecular ash weight (T.A.W.), might be due to the small volume used to measure the trabecular ash density. Luther-1973 investigated the os calcis and first lumbar vertebra of fifty assorted corpses by a Compton backscatter method (Reiss-1973) and by ashing small cylindrical bone samples of approximately $1cm^3$ volume. He found good correlation between the two methods ($r = 0.90$ for the calcaneum and 0.97 for the vertebral body), but very poor correlation between calcaneum and vertebra ($r = 0.28$ for the ash method and $r = 0.31$ for the Compton scattering method). Schneider-1976 using a photon absorptiometric method, demonstrated that the BMC of the calcaneus correlated well ($r = 0.83$) with the BMC of the second lumbar vertebra in ten cases. Schneider ascribed the discrepancy between his results and those of Luther to the fact that calcanei and vertebral are not very homogeneous bones, and to the fact that Luther had taken essentially "point measure-

ments" by both the ash and Compton backscatter methods, while he (Schneider) had taken "average measurements". The same argument would hold in the present study, especially since the punch volume here was only $0.32cm^3$. This might also explain the higher correlations between intact capitate B.A.D. and vertebral P.A.D., since B.A.D. is an average over a larger volume of bone.

4.2 Relations Between Specific Electron Density Measurements and Bone Ash Measurements On Excised Cadaver Bones.

Fundamental to the use of the A.E.C.L. Bone Densitometer as an instrument in vivo monitoring of skeletal mineralization is the requirement that the specific electron density (S.E.D.) measurements it provides be correlated with the amount of trabecular bone at the site of S.E.D. measurement and also the requirement that the trabecular bone at the accessible site measured reflect the status of trabecular bone at the clinically important but inaccessible sites. The experiments with ash measurements discussed in the preceding section indicate that the latter requirement is met only moderately well, but perhaps well enough for clinical decision making so long as no direct measurements of bone mineralization can be made at the inaccessible sites. Therefore, the following investigations were conducted to determine whether the S.E.D. measurements were a good index of trabecular bone mineralization, and whether S.E.D. measurements at an accessible appendicular site could predict trabecular bone mineralization at the inaccessible sites to the degree that such a relationship has been found to exist.

4.2.1 The Relationships Between Specific Electron Density and Ash Density Measurements at Eight Skeletal Sites.

In vitro specific electron density (S.E.D.) measurements were made on eight excised bones from each of ten cada-

vers, and the results compared to ash density measurements made on specimens taken from the S.E.D. measurement sites. The bones consisted of left and right intact capitates, left and right distal radii, distal tibia, femoral neck, and eighth and ninth thoracic vertebrae. All bones, except the capitates, were boiled to remove fat prior to S.E.D. measurement. S.E.D. measurements were made on the A.E.C.L. Bone Densitometer with the bones submerged in a standard depth of water. After S.E.D. measurements, 1cm wide slices were cut from the bones (except the capitates). A $0.32cm^3$ cylinder of trabecular bone (punch volume) was removed from each slice, ashed, and weighed. The punch ash density (P.A.D.) of the punch volume was calculated by dividing the punch ash weight by the punch volume as determined before ashing. The capitates were ashed whole and their bone ash density (B.A.D.) calculated in a similar manner. Table 4.2.1 contains the correlation coefficients between P.A.D. (or B.A.D.) and S.E.D. for several groupings of the bones. The relationships are significant at the 5% level or better for six of the eight bone types, and the correlations ranged from weak, $r = 0.51$ (10) for the tibia, to strong $r = 0.95$ (9) for the femur. Associations between P.A.D. and S.E.D. for larger groups of mixed bone type are significant at the 1% level or better, but only moderately strong. These results indicate that S.E.D. measurements with the AECL Bone Densitometer do indicate tra-

becular bone density but with only moderate accuracy, although the results may be artifactually poor.

Correlations between specific electron density and punch ash density (or bone ash density) varied quite widely over the eight bone types, and on the average correlations were lower than expected. Specific electron density (S.E.D.) correlated best with capitate bone ash density (B.A.D.), r = 0.69 (10) and r = 0.86 (10) for left and right respectively. Coefficients between S.E.D. and P.A.D. for left radius, r = 0.57 (9), and right radius, r = 0.88 (10), and for eighth vertebra, r = 0.68 (9), and ninth vertebra, r = 0.77 (9), are qualitatively similar. Tibial S.E.D. and P.A.D. correlated most poorly, r = 0.51 (10). The high correlation coefficient for femoral S.E.D. versus P.A.D. (r = 0.95, N = 9) is directly attributable to one abnormal specimen which had some compact bone formation in the medullary cavity which drastically increased the S.E.D. and P.A.D. values, thereby increasing the range of values and improving the correlation. Excluding this bone, the correlation coefficient between femoral S.E.D. and P.A.D. drops to r = 0.035 (8). This latter observation suggests that the degree of precision in measuring either S.E.D. or P.A.D., or both; is insufficient for the range of S.E.D. and P.A.D. involved.

Another factor contributing to the lack of strong

TABLE 4.2.1 Correlation coefficients between specific electron density and ash density for all skeletal sites.

	:vs S.E.D. r	(N)
LEFT CAPITATE B.A.D.	0.69	(10)
RIGHT CAPITATE B.A.D.	0.86	(10)
LEFT RADIUS P.A.D.	0.57	(9)
RIGHT RADIUS P.A.D.	0.88	(10)
TIBIA P.A.D.	0.51	(10)
FEMUR P.A.D.	0.95	(9)
8th VERTEBRA P.A.D.	0.68	(9)
9th VERTEBRA P.A.D.	0.77	(9)
CAPITATES ONLY (B.A.D.)	0.76	(20)
APPENDICULAR* P.A.D.	0.64	(29)
AXIAL P.A.D.	0.69	(27)
ALL SITES* P.A.D.	0.63	(56)

*Excluding capitates.

B.A.D. = bone ash density
P.A.D. = punch ash density
S.E.D. = specific electron density

correlation between S.E.D. and P.A.D. may be the difference in size, shape, and location of the measurement volumes involved. The S.E.D. values reflect approximately an $4.7cm^3$ volume, shaped like a diamond rotated about the long axis, and oriented vertically. The P.A.D. results were based on a 0.637cm diameter cylinder one centimeter in length (volume = $0.32cm^3$), oriented horizontally with respect to the S.E.D. volume. Although much care was taken to ensure that the centers of the two volumes coincided, there were inevitably small differences in localization. Further, there is a distinct possibility that the sensitive volume of the AECL Bone Densitometer extended past the limits of the bone when measuring the vertebrae, and perhaps into regions of cortical bone when measuring any of the bones. Since even the density of trabecular bone has been reported to vary considerably at adjacent points at the same site (Luther-73, Schneider-76, Blanton-68), the fact that the A.E.C.L. Bone Densitometer was monitoring a different shape, volume, and perhaps region and type, of bones than contained in the punch volume, some negative effect on correlation between S.E.D. and P.A.D. would be expected.

Still another parameter which might have had a deleterious effect on the strength of the S.E.D. versus P.A.D. association is variation in the composition of the cancellous bone marrow. Even though the bone specimens had been boiled

about eighty minutes to remove any marrow fat and replace it with water (or formalin solution), this process may not have been entirely or uniformally successful, given the differences in shape of the bone specimens. For example, removal of fat from a distal radial metaphysis might have been less successful than from a vertebra. The presence of residual marrow fat would result in a lower measured S.E.D. value, but would not affect the P.A.D. value in any way, tending to destroy the relationship.

Finally, the S.E.D. result is not entirely free from the effects of material surrounding the volume of matter measured. The configuration and thickness of the cortical bone enclosing the trabecular bone in a vertebra is quite different from that at the femoral neck, decreasing the S.E.D. versus P.A.D. correlation further.

Notwithstanding the above source of random and systematic error, there is a significant relationship between S.E.D. and P.A.D. as measured in this study. The correlation coefficient between S.E.D. and P.A.D. for all sites except the capitates was $r = 0.63$, $N = 56$, and was significant at the 1% level. Correlation coefficients based on other smaller groupings were qualitatively similar: for all appendicular sites except capitates, $r = 0.64$, $N = 29$, and for all axial sites, $r = 0.69$, $N = 27$. Figure 4.2.1 is a scattergram of P.A.D. versus S.E.D. for all sites except the capitates.

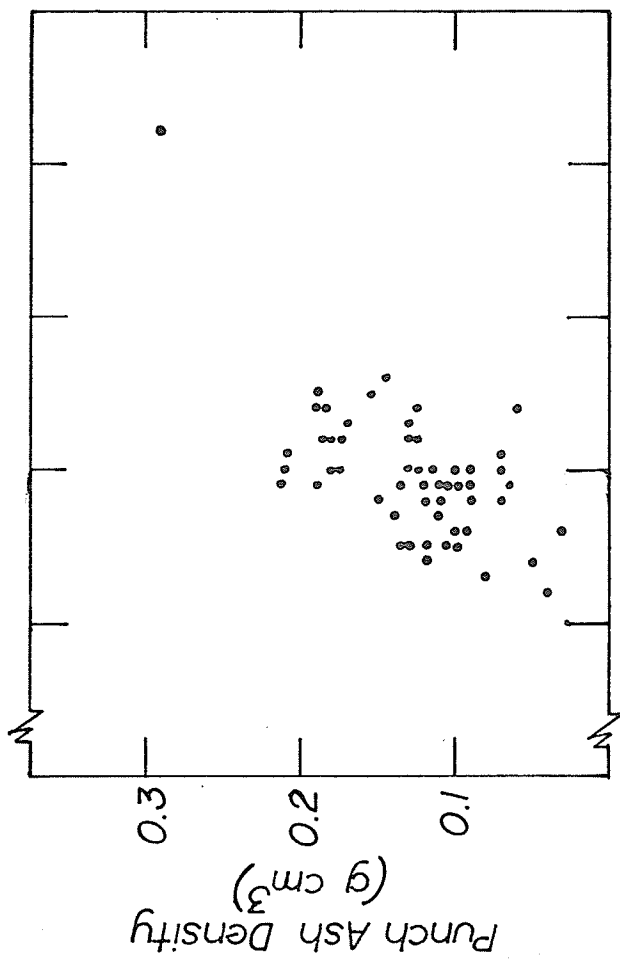

Figure 4.2.1 Scattergram between punch ash density for left and right radii, right tibia and femur, and eighth and ninth thoracic vertebrae.

4.2.2 The Relationships Between Specific Electron Density Measurements at Accessible Skeletal Sites and Ash Measurements at Inaccessible Skeletal Sites.

The A.E.C.L. Bone Densitometer prototype was designed for the purpose of measuring trabecular bone density at an accessible appendicular site and thereby to predict the status of bone mineralization at the clinically important, but practically inaccessible, axial and femoral neck sites. The possibility of such an application was investigated by measuring the specific electron density of the left and right capitates, left and right distal radial metaphyses, and distal tibial metaphysis, and comparing these results to ash densities of mixed-bone and trabecular bone specimens from the femoral neck and eighth and ninth vertebrae. The correlation coefficients which appear in table 4.2.2 were compared to ash measurement correlations between corresponding sites (table 4.1.2). Data for the capitates was fairly parallel in all respects, data for the tibia differed with respect to the femoral neck correlations, and data for the radii was quite variable. The results of this study indicate that, for the degree of association thought to exist between accessible appendicular trabecular bone sites and clinically important but inaccessible skeletal sites, specific electron density measurements of the capitate are a good predictor of vertebral mineral status, but no appendicular S.E.D. measurement is a good predictor of femoral neck mineralization.

There appears to be as significant a relationship between capitate S.E.D. and vertebral P.A.D., r = 0.68 (9) to r = 0.82 (9), as between capitate B.A.D. and vertebral P.A.D., r = 0.68 (9) to r = 0.77 (9), but other comparisons are doubtful. Radial S.E.D. versus vertebral P.A.D., r = 0.51 (9) to r = 0.68 (9), is improved somewhat over radial versus vertebral P.A.D., r = 0.14 (9) to r = 0.44 (9), but the small sample size precludes a firm conclusion as to whether a real relationship exists between radial and vertebral trabecular bone mineralization. All of the associations between appendicular S.E.D. and femoral neck P.A.D., r = 0.01 (8) to r = 0.41 (8), are much worse than the corresponding P.A.D. (or B.A.D.) versus femoral neck P.A.D. relations, r = 0.29 (8) to 0.68 (7), again without a systematic explanation. The distal tibia would appear to be the poorest appendicular site at which to measure S.E.D. for the purpose of predicting vertebral mineralization since correlation coefficients are r = 0.20 (9) and r = +0.28 (9) for S.E.D. versus P.A.D. relationships, and r = 0.10 (9) and r = -0.13 (9) for P.A.D. versus P.A.D. relationships.

TABLE 4.2.2 Correlation coefficients between S.E.D. at accessible skeletal sites and P.A.D. at inaccessible skeletal sites.

	FEMUR P.A.D.	9th Vertebra P.A.D.	9th Vertebra P.A.D.
Left Capitate SED	(0.383 (8))	0.68 (9)	0.69 (9)
Right Capitate SED	(0.41 (8))	0.81 (9)	0.82 (9)
Left Radius SED	0.10 (7)	0.68 (9)	0.51 (9)
Right Radius SED	0.26 (8)	0.59 (9)	0.51 (9)
Tibia SED	0.01 (8)	0.20 (9)	0.28 (9)

4.3 Relations Between Absorptiometric Bone Mineral Measurements and Bone Ash Measurements on Excised Cadaver Bones.

Since comparatively little data regarding Compton scattering methods of bone density measurement in vitro has been published, and since much valid data utilizing the absorptiometric method of in vitro and in vivo bone mineral measurement is available, the latter was used as a control for the present study. Eight bone specimens from ten cadavers were measured under the same experimental conditions using the A.E.C.L. Bone Densitometer and the Norland-Cameron Bone Mineral Analyzer, and both sets of results compared to subsequent ash measurements of the bone specimens. This chapter deals with the comparison of the Norland-Cameron Bone Mineral Analyzer results with the bone ash measurements.

Absorptiometric bone mineral measurements were made with a Norland-Cameron Bone Analyzer (B.M.A.) at trabecular sites on eight bone specimens excised from each of ten cadavers, and the results compared to bone ash measurements of slices cut from the specimens at the same sites. Bone mineral content (BMC), in g/cm, and bone mineral content per bone width (BMC/BW), in g/cm^2, were determined at sites of maximum trabecular bone on left and right capitates, left and right distal radial metaphyses, distal tibial metaphysis, femoral neck and eighth and ninth thoracid vertebrae. All bone

specimens except the capitates had been boiled about eighty minutes to remove marrow fat prior to B.M.A. measurements. The volumes of the capitates were determined, the intact capitates ashed, and capitate bone ash weight (B.A.W.) and bone ash density (B.A.D.) determined. One centimeter long slices, centered on the scan path of the BMC measurements, were cut from all other bone specimens. Slice volumes were measured, the slices ashed, and slice ash weights (S.A.W.) and slice ash densities (S.A.D.) determined. Trabecular ash was separated from each ashed slice, weighed, and the trabecular ash weight (T.A.W.) calculated. Trabecular ash density was not determined due to the large uncertaintes involved in estimating trabecular volumes.

Correlation coefficients between B.M.A. measurements and ash measurements appear in table 4.3.1. Individual correlations between BMC and S.A.W. were all significant at the 1% level or better, and coefficients ranged from $r = 0.915$ to $r = 0.988$ for $N = 9$ or 10. The somewhat lower coefficients, $r = 0.64$ (10) and $r = 0.81$ (10) between capitate BMC and B.A.W. is understandable since the whole bone was ashed, and not the one centimeter slice to which the Bone Mineral Analyzer is calibrated. The correlation coefficient between BMC and S.A.W., taking the accessible sites as a group, but excluding the capitates, was $r = 0.99$ (27), and was identical to that for the inaccessible sites as a group, $r = 0.99$ (27). When all

the slice sites were considered together, the coefficient was r = 0.99 (56). These findings compare favourably with those of other investigators (Mazess, Ort, Judy, Mather - 1970, Mazess, Cameron, Miller - 1970). The results indicate that the Norland-Cameron Bone Mineral Analyzer indeed measures the mineral content of a one centimeter long slice of bone centered on the scan path. They also verify that the ashing technique employed was valid for use in evaluation of the specific electron density measurements of the A.E.C.L. Bone Densitometer, the subject of this thesis.

The relationships between BMC/BW and ash density are included because BMC/BW has been reported useful in reducing the variability in normative data (Smith-70). Although all of the correlation coefficients listed in table 4.3.1 (b) for ash density versus BMC/BW significant at the 1% level, they are in general slightly lower, (r = 0.78, N = 10 to r = 0.95, N = 10) than the corresponding ones for ash weight versus BMC noted above. The exceptions are the coefficients for the capitates. Considering all the accessible sites, except the capitates as a group, the correlation coefficient between S.A.D. and BMC/BW is r = 0.80 (28), which is markedly lower than that for the inaccessible sites taken as a group, r = 0.92 (27). The overall correlation considering both accessible and inaccessible sites (excluding the capitates) was quite strong r = 0.90 (55).

Since changes in an individual's bone mineral status have been shown to occur earlier, or to a more marked degree, in trabecular bone (Dalen-1973, Smith-1973, Goldsmith-1971) it is also appropriate to investigate the relationship between bone mineral analyzer measurements and trabecular ash weights. Table 4.3.1 (c) lists the coefficients for BMC and BMC/BW versus T.A.W. according to bone slice site, along with the percentage trabecular bone at the site. As might be expected, the strength of the BMC versus T.A.W. relationship is directly proportional to the percentage of trabecular bone. Thus the search for a radial BMC measurement site containing more trabecular bone than the original radial midshaft site is justified. However, the Bone Mineral Analyzer is not well suited for measuring the radial metaphysis in vivo (Johnston-1970), although some methodologies make this possible (Nilsson-1973), Dalen & Jacobson-1973). Rather, the 1/10 distal radius site, or thereabouts, has often been preferred for clinical studies (Johnston-1970, Smith-1973, Schlenker-1973, Meuller-1976). However, the percentage of trabecular mass (%T.M.) changes rapidly from a point one centimeter from the radial styloid, %T.M. = 53%, to a point three centimeters from the radial styloid, %T.M. = 13% (Schlenker-1976). Comsequently repositioning errors (Panel Discussion-1974) and increased biological variation (Dalen-1973) make this quest self-limiting, unless a precise localizing method is developed, per-

haps such as discribed in Wing-1974. Further, as evidenced by the BMC/BW versus T.A.W. correlation coefficients in table 4.3.1 (c), normalizing to bone width reduces the strength of the relationships at accessible sites. It was this dilemma which the A.E.C.L. Bone Densitometer was designed to overcome.

TABLE 4.3.1 Correlation coefficients between Bone Mineral Analyzer Measurements and Ash Measurements of excised cadaver bones.

(a) Correlation coefficients between bone mineral content (BMC) and slice ash weight (S.A.W.) for composite bone specimens.

	:vs. BMC r	(N)
LEFT CAPITATE* B.A.W.	0.63	(10)
RIGHT CAPITATE* B.A.W.	0.81	(10)
LEFT RADIUS S.A.W.	0.95	(9)
RIGHT RADIUS S.A.W.	0.92	(10)
TIBIA S.A.W.	0.96	(10)
FEMUR S.A.W.	0.96	(10)
8th VERTEBRA S.A.W.	0.99	(9)
9th VERTEBRA S.A.W.	0.95	(9)
ACCESSIBLE** S.A.W.	0.99	(29)
INACCESSIBLE** S.A.W.	0.99	(56)
ALL SLICES** S.A.W.	0.99	(56)

(b) Correlation coefficients between bone mineral content per bone width (BMC/BW) and slice ash density (S.A.D.) for composite bone specimens.

	:vs. BMC/BW r	(N)
LEFT CAPITATE* B.A.D.	0.88	(10)
RIGHT CAPITATE* B.A.D.	0.95	(10)
LEFT RADIUS S.A.D.	0.90	(10)
RIGHT RADIUS S.A.D.	0.78	(10)
TIBIA S.A.D.	0.80	(10)
FEMUR S.A.D.	0.94	(9)
8th VERTEBRA S.A.D.	0.95	(9)
9th VERTEBRA S.A.D.	0.87	(9)
ACCESSIBLE** S.A.D.	0.80	(28)
INACCESSIBLE** S.A.D.	0.92	(27)
ALL SLICES** S.A.D.	0.91	(55)

*Capitate values are for total bone.

**Capitate values not included.

TABLE 4.3.1 (c) Correlation coefficients between Bone Mineral Analyzer measurements and trabecular ash weight (T.A.W.) of bone slices.

	BMC vs T.A.W. r	(N)	BMC/BW vs T.A.W. r	(N)	Mean Percent Trabecular Bone Mass per Slice
Right Radius	0.890	(10)	0.732	(10)	60.6%
Left Radius	0.839	(9)	0.621	(9)	59.9%
Tibia	0.769	(10)	0.594	(10)	57.6%
8th Vertebra	0.712	(8)	0.950	(8)	52.8%
9th Vertebra	0.638	(8)	0.926	(8)	52.7%
Femoral Neck	0.531	(8)	0.075	(8)	42.9%

4.4 Effects of Marrow Fat on Bone Mineral Measurements of Trabecular Bone Specimens.

The effect of marrow fat on bone mineral measurements with the AECL Bone Densitometer and the Norland-Cameron Bone Mineral Analyzer (B.M.A.) was investigated by measuring fifty excised cadaver bones both before and after boiling them. Bone Densitometer measurements of specific electron density (S.E.D.) increased by an average of 7% as a result of boiling, and BMA measurements of bone mineral content (BMC) increased by an average of 10%. Analysis of the results indicates that S.E.D. measurements of trabecular bone are more likely to monitor marrow fatdeposition than trabecular bone loss, and that BMC measurements may be in error by as much as 22% at the distal radial metaphysis.

Five bones excised from each of ten embalmed cadavers were measured as described in sections 2.1.3 and 2.2.3. The bones included left and right distal radial metaphyses, the eighth vertebra, one tibia, and one femoral neck. Specific electron density (S.E.D.) and Bone Mineral Content (BMC) measurements were made before and after boiling the specimens for about 80 minutes to remove marrow fat. Immediately after boiling, the bone specimens were replaced in 10% formalin solution, and were stored thus until measured. Upon cooling formalin solution would presumably fill the marrow space vacated by the fat.

Four replicate measurements were averaged to obtain each S.E.D. and BMC value. The pre-boiling values were divided by the post-boiling values and the mean ratios for each bone are given for S.E.D. and BMC in table 4.4.1. Post-boiling data was not available for two of the eight vertebrae.

The effects of marrow fat were slightly more marked on the BMC measurements than on the S.E.D. measurements, and more severe for the eighth vertebrae than for the other bone specimens. The mean S.E.D. ratios ranged from 0.909 for the eighth vertebra to 0.952 for the tibia, while ranges for the BMC ratios were 0.870 to 0.952, respectively. Individual values used to complie each of the mean ratios varied even more widely, ranging from 0.714 to 1.009 for S.E.D. measurements of the eighth vertebra and from 0.702 to 1.000 for BMC of the eighth vertebra. Thus errors as great as 29% were observed in individual S.E.D. measurements and as great as 30% in individual BMC measurements. It is questionable whether marrow fat alone could cause such low values as were observed in some cases, and other influences might be suspected, such as gas deposits produced by decaying marrow, or air introduced during fixation of the bone specimens to the acrylic mounting sheets.

The mean ratios for the distal radial metaphysis are of special interest, since this was the in vivo site used for S.E.D. measurements in the present adult clinical study, and has been used for in vivo BMC measurements as well (Nilsson-1973).

The mean error in BMC was about 6.5% which is quite close to that calculated by Sorenson-1973 (5%), for trabecular bone in which 50% of the volume is fat. Presumably, therefore, trabecular marrow fat is commonly 50% or more of the marrow volume in the cases under investigation here. Similar theoretical calculations for S.E.D. measurements have not been found in the literature, and so a rough analysis of the situation follows.

Consider a specimen of trabecular bone of overall density D_s, containing trabeculae of density D_t and marrow of density D_m. Then if the fraction of the specimen occupied by the trabeculae is F_t, the density of the specimen is given by

$$D_s = D_t F_t + (1 - F_t) D_m \quad \text{. . . . . eq. 4.4.1}$$

Consider further the composition of normal read bone marrow, with its inorganic, organic and water constituents. If fat is also present, it replaces water in marrow cells, so the fractional volumes of fat and water are complimentary. The density D_m of marrow, then, is given by

$$D_m = D_i F_i + D_o F_o + D_w F_w + D_f F_f \quad \text{. . . . eq. 4.4.2}$$

in which "i" refers to the inorganic compoents, "o" refers to the organic components, "w" refers to the water component, and "f" refers to the fat component of the marrow. Table 4.4.1 lists the densities and the fractional volumes of the various constituents of normal cancellous bone. Substituting for D_i,

F_i, D_o, F_o, D_w, and D_f from Table 4.4.1, the expression for marrow density becomes

$$D_m = 1.0384 - 0.1\ F_f \quad \text{eq. 4.4.3}$$

Substituting this equation into equation 4.4.1, along with the numerical value for D_t from the table, the expression for specimen density becomes

$$D_s = 0.8616\ F_t + 0.1\ F_f\ (F_t - 1) + 1.0384 \quad \text{eq. 4.4.4}$$

There are five cases which might now be considered:

(i) There is no fat in the marrow and the specimen density is $D_s(i) = 1.09 g/cm^3$ as quoted by (Blanton-1968).

$F_f = 0$, and from equation 4.4.4, $F_t = 0.0599$. In otherwords, about 6% of cancellous bone volume is occupied by trabeculae under ideal circumstances.

(ii) There is no fat in the marrow, but there is a 30% decrease in bone mineral and replaced by marrow. Then $F_f = 0$, $F_t = 0.0419$, and $D_s(ii) = 1.075 g/cm^3$. The ratio $D_s(ii)/D_s(i) = 0.986$ which represents only a 1.4% decrease in trabecular bone density for a 30% decrease in bone mineralization!

(iii) There is no demineralization, but there is an 18% infiltration of marrow fat. Thus $F_t = 0.0599$ and $F_f = 0.1645$ and $D_s(iii) = 1.075 g/cm^3$. The ratio $D_s(iii)/D_s(i) = 0.986$

which equals that for case (ii). Consequently, an 18% infiltration of marrow fat causes the same decrease in cancellous bone density as a 30% demineralization!

(iv) There are no trabeculae, and there is no fat. Then $F_t = 0$, and $F_f = 0$, $D_s(iv) = 1.038 g/cm^3$ and $D_s(iv)/D_s(i) = 0.953$. Therefore complete trabecular demineralization would lead only to a 5% decrease in density!

(v) There are no trabeculae, and all the water is replaced by fat. This is a hypothetical case to determine the minimum conceivable density. Thus, $F_t = 0$, $F_f = 0.91$, $D_s(v) = 0.95$. It might be noted here that a number of in vitro and in vivo specific electron density measurements produced values as low as 0.95.

TABLE 4.4.1 Mean bone mineral measurements ratios (pre-boiling to post-boiling) for four types of excised cadaver bones.

BONE (N)	MEAN S.E.D. Ratio (Range)	MEAN BMC RATIO (Range)
RADIUS (20)	0.926 (0.778 to 0.995)	0.935 (0.845 to 1.002)
8th VERTEBRA (8)	0.909 (0.714 to 1.009)	0.870 (0.702 to 1.000)
TIBIA (10)	0.952 (0.780 to 1.018)	0.952 (0.829 to 1.005)
FEMORAL NECK (10)	0.952 (0.845 to 1.028)	0.952 (0.746 to 0.991)

TABLE 4.4.2 Constituents of cancellous bone, and some of their values.

CONSTITUENTS	DENSITY (g/cm^3)	FRACTIONAL VOLUME
Trabecuae (Marrow-free)	1.9	F_t*
Marrow		
- inorganic	3.0	0.002
- organic	1.41	0.084
- water	1.00	$0.914-F_f$*
- fat	0.90	F_f*
Cancellous bone (embalmed, mean value)	1.09	1.000

*see text for explanation.

CHAPTER 5

In Vivo Monitoring of Bone Mineral Status In the Legs of Paraplegic Children Receiving Standing Therapy.

The A.E.C.L. Bone Densitometer and the Norland-Cameron Bone Mineral Analyzer were used to monitor bone mineral status in the legs of a group of paraplegic children undergoing standing therapy. A cross-sectional study was performed in which the developement of bone with age was investigated and the results compared to similar studies in a group of normal children of similar age. A longitudinal study was also performed to study the effect of the standing therapy on tibial bone mineralization.

There were eight children in the paraplegic group and seven children in the normal control group. The paraplegic group comprised seven menigomyelocele children and one child paralyzed due to spinal cord trauma. There were six boys ranging in age from 20 months to 37 months at first measurement, and two girls aged 73 to 104 months. The control group consisted of three boys aged 36 to 60 months and four girls aged 30 to 60 months.

Six of the paraplegic children were measured twice, once prior to commencing therapy and once again after $5\frac{1}{2}$ to 10 months of standing therapy, and the remaining two were

measured only once, prior to therapy. The specific electron densities (S.E.D.) of both distal tibial metaphyses were measured with the A.E.C.L. Bone Densitomer (B.D.) at sites selected by inspection of x-rays of the lower limbs. Bone mineral content (BMC) and bone width (BW) of the midshaft and distal tibia were measured to both legs using the Norland-Cameron Bone Mineral Analyzer (BMA). Bone mineral content per bone width (BMC/BW) was calculated in each case. In all instances on both instruments, four replicate measurements were taken and the results averaged.

Bilateral anterior-posterior (AP) and lateral x-rays of the ankles were taken of the paraplegic children to aid in localizing the distal tibia metaphyses of S.E.D. measurements. For the AP projection, lead markers were placed at the medial and laterial malleoli of the tibia. For the lateral projection, lead markers were placed at the medial malleolus and 3 inches proximal to fit. All exposures were made using a focal-to-film distance of 40 inches to reduce magnification. Non-screen mammography film was used without an intensifying screen for fine-detail technique. All x-rays were taken by the same technologist to ensure consistent technique.

Bone mineral analyzer (BMA) measurements of the paraplegic children were made at an area of predominantly cortical bone over the midshaft of the tibia, and at an area with a good proportion of cancellous bone over the distal aspect of

the tibia in the region of the metaphysis. Measuring the length of the tibia from the medial malleolus to the medial joint line, scams were ,ade at $\frac{1}{4}$ and $\frac{1}{2}$ the distance. These sites were termed the "$\frac{1}{4}$ distal tibia" and "tibial midshaft" sites, respectively. The foot and knee were oriented upward for all BMC scans.

The normal children were measured at three skeletal sites using only the Bone Mineral Analyzer. Bone mineral content (BMC) and bone width (BW) were determined in the left leg at the $\frac{1}{2}$ and $\frac{1}{4}$ tibial sites (as defined for the paraplegic children) and also at the left mid-radius. The mid-radius site was taken as one third the distal from the ulnar styloid process to the olecranon. Four scans were made at each site and the results averaged. The mid-radial site was measured in order to compare the normal children data to published normative data (Mazess and Cameron-1973, Klem-1976, Exner-1979).

Bone Mineral Analyzer measurements in the normal group were used to calculate the average change in BMC and BMC/BW with age (% change per month) at each of the three sites measured. Percent changes per month appear in Table 5.1 (a) and were calculated by dividing the slope of the linear regression line of each index versus age by the mean index for the group, and multiplying by one hundred. Both sexes were taken as a group since other investigators have concluded that

no significant difference in bone growth rate is demonstrated between boys and girls up to the age of puberty (Mazess and Cameron-1973, Exner-1979). The mid-radius and $\frac{1}{2}$ distal tibia sites showed equal growth rates of cortical bone when corrected for bone width, +0.86% per month for the radius and +0.87% per month for the tibia. This works out to about 10% per year which is considerably higher than the 4% annual change quoted by Mazess and Cameron-1973. The discrepancy may be due to the small sample size or to the younger age group in the present study. The growth rate observed at the more trabecular $\frac{1}{4}$ distal tibia site is about double that at the cortical bone sites, with a change in BMC/BW of about +1.89% per month or 21% annually. This rate compares well with the 20% per year increase in BMC/BW of the os calcis apparent in the data by Klemm-1976 for a study of 137 children between four and twenty years of age. Because of its seemingly greater sensitivity, the $\frac{1}{4}$ distal tibial site was chosen for judging the effects of standing therapy in the group of paraplegic children.

The growth rates indicated by the Bone Mineral Analyzer (BMA) indices in the legs of the paraplegic children prior to therapy were much below those for the normal group. Percent changes in BMA indices per month are presented in Table 5.1 (b), and were calculated as for the normal group except that they are based on average values for left and right leg values

TABLE 5.1 Changes in bone mineral measurements as a function of age in normal and paraplegic children

(a) Normal children

	1/3 DISTAL RADIUS		1/2 DISTAL TIBIA		1/4 DISTAL TIBIA	
	BMC	BMC/BW	BMC	BMC/BW	BMC	BMC/BW
Change in Index with age (% per month)	+1.13	+0.86	+1.50	+0.87	+1.92	+1.78

(b) Paraplegic children

	DISTAL TIBIAL METAPHYSIS	1/2 DISTAL TIBIA		1/4 DISTAL TIBIA	
	S.E.D.	BMC	BMC/BW	BMC	BMC/BW
Change in Index with age* (% per month)	-0.111	+0.79	_0.52	+0.63	+0.34

*Based on average of left and right leg values in each cases

TABLE 5.2 Changes in mean* bone mineral indices in the tibiae of 6 paraplegic children undergoing standing therapy.

	DISTAL TIBIAL METAPHYSIS	1/2 DISTAL TIBIA		1/4 DISTAL TIBIA	
	S.E.D.	BMC	BMC/BW	BMC	BMC/BW
Change in Index with Age* (% per month)	+0.25	+1.53	+1.21	+1.09	+1.09

*Based on average of left and right leg values in each case.

prior to therapy. The BMC/BW growth rates for the cortical ($\frac{1}{3}$ distal tibia) site showed a greater change with age (0.52% /month) than did those for the trabecular ($\frac{1}{4}$ distal tibia) site (0.34%/month), which differs from the normal group. However, age relationships for all indices were well below corresponding values in the normal group.

Changes in specific electron density (S.E.D.) at the distal tibial metaphysis of the paraplegic children as a function of age could not be compared with normal values directly, but indirect comparisons with published data may explain the observed results. The correlation of S.E.D. with age was negative (-0.111% per month) suggesting a progressive decrease in density of trabecular bone at the distal tibial metaphysis. However, one low S.E.D. value for the oldest child causes the negative change. Without this value, the change in S.E.D. with age is 0.0014% per month, which is essentially nothing. This would seem reasonable since Exner-1979, using an I-125 gamma CAT scanning method, observed that trabecular bone density at the distal radius was independent of age and sex in the age range 4 to 40 years. On the other hand, Klemm-1976, using a modified Cameron absorptiometric method, reports an annual growth rate of about $4\frac{1}{2}$ percent for bone density of the os calcis, but almost certainly some cortical bone was included in his values. Consequently, S.E.D. measurements of trabecular bone would seem a relatively poor index of bone

mineral status for cross sectional studies of different age populations.

Results of the longitudinal study to determine the effects of standing therapy on tibial bone mineralization were positive in all instances, but BMA indices were markedly more sensitive in monitoring changes than the S.E.D. index. Figure 5.1 (a) is a plot of BMC/BW at the $\frac{1}{4}$ distal tibia against time illustrating the individual changes occuring with therapy, and figure 5.1 (b) shows a similar plot of S.E.D. versus time. The average change (% per month) during therapy for the five indices of tibial mineralization are given in table 5.2. They are based on averages for left and right legs, and were calculated as before. The fact that the mean changes in BMA indices at the $\frac{1}{3}$ distal tibia (cortical) site are greater than those at the $\frac{1}{4}$ tibia (trabecular) site is explained, unless it is an artifact due to the small sample. More important in any case is the fact that BMC (and BMC/BW changes (%/month) during therapy were approximately two to three times as great as expected due to age alone. Since S.E.D. changes (%/month) were only one sixth to one quarter the magnitude of BMC and BMC/BW changes, specific electron density is obviously markedly less sensitive to small changes in tibial bone mineralization in comparison to the BMA indices.

Analysis of the data indicates that the bone mineral development in the legs of the paraplegic children was below

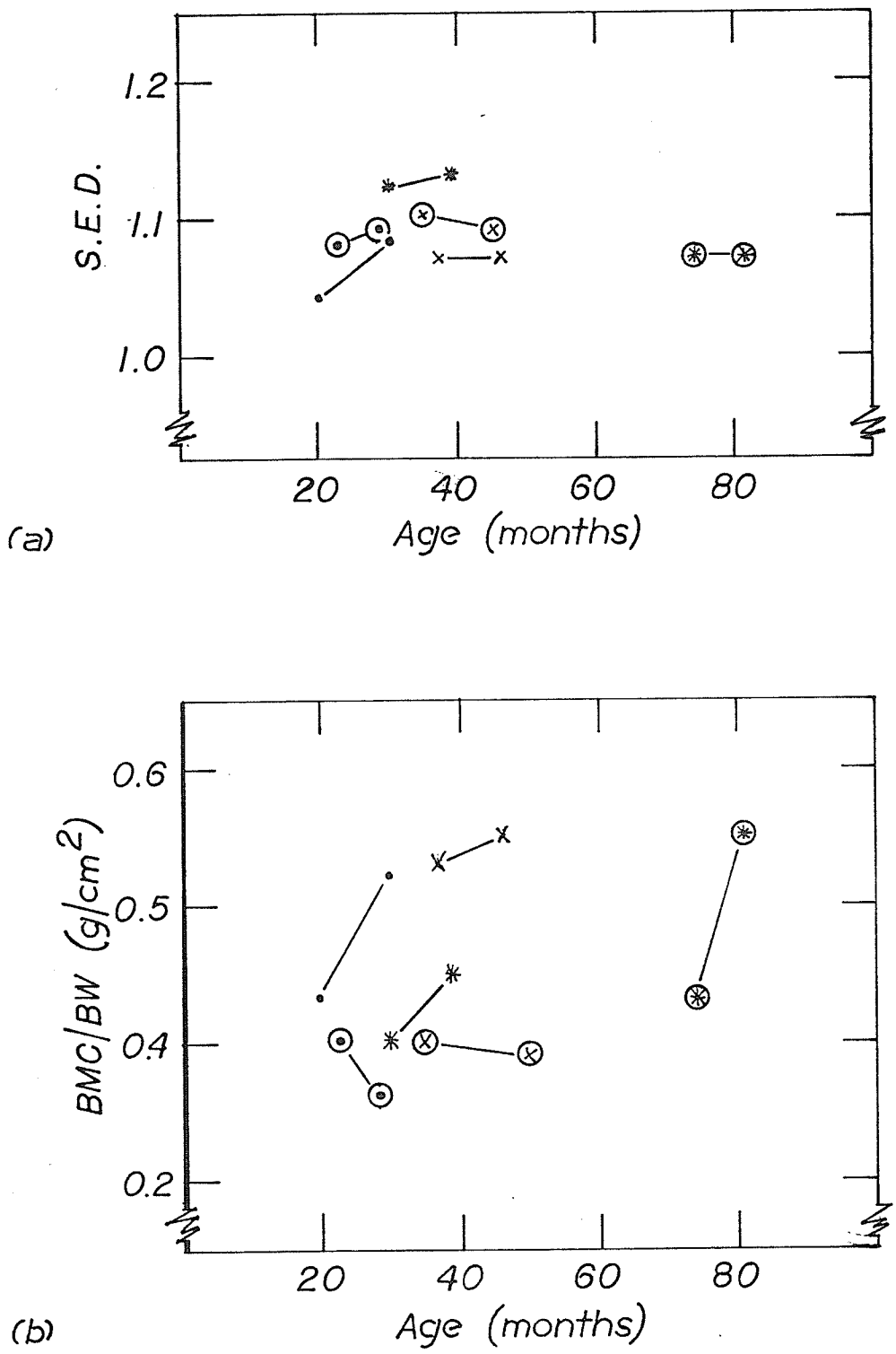

Figure 5.1 Plot of tibial bone mineral measurements against time for six paraplegic children before and after standing therapy.

normal prior to embarking on standing therapy, and that, on the average, it increased to about normal after therapy. These conclusions were based on the Bone Mineral Analyzer data of the paraplegic and the normal groups, and on published normative statistics. The Bone Densitometer results are more difficult to interpret since S.E.D. measurements were not performed on the group of normal children. However, it is evident that S.E.D. of the tibial metaphysis is not as sensitive an index of bone mineral growth as BMC/BW at the $\frac{1}{4}$ distal tibia. These results corroborate those in the literature.

CHAPTER SIX

In Vivo Monitoring of Bone Mineral Status in Adult Females with Metabolic Bone Disease.

The bone mineral status of twenty-seven adult female patients with clinically diagnosed metabolic bone disease was investigated using the Norland-Cameron Bone Mineral Analyzer and the A.E.C.L. Bone Densitometer. The patients comprised three different clinical groups, and a cross-sectional study was performed on each group to determine the changes in the various measured bone mineral indices as a function of age. Bone Mineral Analyzer (BMA) results were compared with published normative data and Bone Densitometer results were compared to B.M.A. results. Bone Mineral Analyzer results correlated well with the clinical situation in each group, but the Bone Densitometer results did not.

The patients ranged in age from 43 to 89, and fell into three clinical groups. Twelve women had been started on steroid therapy for rheumatoid arthritis, nine suffered from post-menopausal osteoporosis, and five were hypoparathyroid.

Bone mineral status was assessed at two points in each radius using the Bone Mineral Analyzer (BMA), and at one point in each radius using the Bone Densitometer (B.D.).

B.M.A. measurements consisted of bone mineral content (BMC) and bone mineral content per bone width (BMC/BW) at the 1/3 and 1/10 distal radial sites, determined by measuring 1/3 and 1/10 the distance from the ulnar styloid process to the olecranon, respectively. Specific electron density (S.E.D.) was measured with the Bone Densitometer at the distal radial metaphysis, which was identified by the palpation of the distal radial tubercle. Four replicate measurements were made at each site, and the results averaged.

The data generated in the study were analyzed from two points of view. First, the rate of change of each bone mineral index as a function of age was calculated. The percent change in the index per year (%/yr.) was taken to be the slope of the linear regression line (of the index versus age), divided by the mean value of the index for the group, and multiplied by one hundred. The rates of change were calculated for (S.E.D.) measurements at the distal radial metaphysis site, and for BMC and BMC/BW measurements at the 1/3 and 1/10 distal radial sites. Comparisons were made between the rates of change of bone mineral as determined by the two instruments, and as published for normal populations. Secondly, the osteoporotic and the hypoparathyroid groups were compared to determine whether their populations could be distinguished from each other by mean absolute values of the various bone mineral indices. Group means were calculated

for the 1/3 and 1/10 radius BMC and BMC/BW values, and for radial metaphysis S.E.D. values. Data for left and right arm were pooled in all cases, to obtain a better average value for each person. This seemed justified since many investigators (Shapiro-1973, Nilsson-1973, Exner-1979) have reported no significant difference between bone mineralization of the dominant and non-dominant arms. A t-test was used to determine the significance of the difference between group means for each index. The statistics generated in these analyses are presented in tables 6.1, 6.2, and 6.3.

Analysis of the rates of change of bone in the three clinical groups indicates that the specific electron density (S.E.D.) of the distal radial metaphysis is not as sensitive an index as are bone mineral content (BMC) and bone mineral content per bone width (BMC/BW) measured at either the 1/3 or the 1/10 distal radial site. In the rheumatoid arthritis, steroid therapy (S.T.R.A.) group, all of the Bone Mineral Analyzer (B.M.A.) indices showed a net loss in bone mass with age (-0.33%/yr. to -1.17%/yr.). Normal rates of bone mineral loss determined at the same sites and by the same method were reported by Mazess and Cameron-1973 for the same age range (50 - 89 years), and show slightly higher rates of loss (-0.70%/yr. to -1.04%/yr.) on the average. This difference in bone loss rates between the present STRA group and normals is probably due only to the small sample (12

TABLE 6.1 Rates of change in bone mineral indices in three clinical groups of adult females.

GROUP (N) (Age Range)	STATISTIC	DISTAL RADIAL METAPHYSIS S.E.D.	1/3 DISTAL RADIUS BMC	1/3 DISTAL RADIUS BMC/BW	1/10 DISTAL RADIUS BMC	1/10 DISTAL RADIUS BMC/BW
Rheumatoid Arthritis	Rate of Change in Index for Group	+0.24%/yr.	-0.63%/yr.	-1.17%/yr.	-0.33%/yr.	-0.45%/yr.
(12) (56-89 yrs.)	Rate of Change in Index for Normals*	---------	-0.91%/yr.	-0.93%/yr.	-1.04%/yr.	-0.70%/yr.
Post-Menopausal Osteoporosis	Rate of Change in Index for Group	-0.14%/yr.	-1.34%/yr.	-2.48%/yr.	-1.90%/yr.	-4.45%/yr.
(a) (43-73 yrs.)	Rate of Change in Index for Normals*	----------	-1.13%/yr.	-1.07%/yr.	-0.99%/yr.	-0.82%/yr.
Hypoparathyroid	Rate of Change in Index for Group	+0.08%/yr.	+0.40%/yr.	+0.53%/yr.	+0.10%/yr.	+0.12%/yr.
(5) (36-64 yrs.)	Rate of Change in Index for Normals*	---------	-0.83%/yr.	-0.72%/yr.	-0.71%/yr	-0.97%/yr.

*Normal values calculated from data taken from Mazess and Cameron - 1973.

patients) in the present study. In any case, in view of data reported by Mueller-1973, one would not necessarily expect a greater than normal rate of loss in the present STRA group, since these women had just been started on corticosteroid therapy, and were assorted as to severity and duration of the arthritic disease. Mueller found that, although the decline in BMC was clearly related to the duration of rheumatoid arthritis, it was significantly greater than normal only after three years of corticosteroid therapy, and only after fifteen years in untreated cases of arthritis. Further, Mueller did not discern any differences in rates of bone loss between the 1/3 radius and 1/10 radius measurement sites. Therefore, the slightly higher rates of loss in the present study which are noted at the 1/3 radius site compared to the 1/10 radius site are also probably not significantly different. However, the rate of change of radial metaphyseal S.E.D. was positive, which is contrary to the findings with the Bone Mineral Analyzer, but not entirely surprising. Exner-1979 found no change in distal radial trabecular bone density with age in a normal population, so the small rate of increase in S.E.D. (0.24%/yr.) observed in the present study is not inconsistent with what might be expected.

A similar analysis of the post-menopausal osteoportic and hypoparathyroid groups also demonstrates the superiority of the Bone Mineral Analyzer over the Bone Densito-

meter as a diagnostic aid in these clinical conditions. In the osteoporotic (OP) group, BMC and BMC/BW at both the 1/3 and the 1/10 distal radius sites showed rates of demineralization (-1.34%/yr. to -4.45%/yr.) that were markedly in excess of normal rates (-0.82%/yr. to -1.07%/yr.) for the same age group, 43 to 73 years. Also the 1/10 distal radius site showed a much greater rate of bone loss than the 1/3 distal radius site, which is in keeping with the findings of Wahner-1973. The fact that radial metaphyseal S.E.D. readings showed a decline (-0.14%/yr.) is overshadowed by the fact that the value is quite small in comparison to the B.M.A. indices, and the fact that this result could easily be due to random error, given the possibility that trabecular bone density remains constant with age (Exner-1979).

In the hypoparathyroid group, the rate of loss of bone mineral with age would be expected to be less than normal. This was indeed the case in this study, since the rates of change for all the bone mineral indices were positive as a function of age. Although the rates of change of BMC and BMC/BW were only slightly positive (+0.10%/yr. to +0.53%/yr.), this is probably significant since it is a marked departure from the normal demineralization rates (-0.71%/yr. to -0.97%/yr.) for the same age group, 36 to 64 years. Again, although the S.E.D. change rate is slightly positive (+0.08%/yr.), it might be expected to be zero (Ex-

ner-1979), and the result is in all liklihood due to random influences on the measurement.

The two most diverse clinical groups were chosen for the purpose of comparing group bone mineral index means by the t-test (Sokal-1973). The osteoporotic group mean was compared to the corresponding hypoparathyroid group mean for each of the five bone mineral indices. Table 6.3 contains the calculated t-values. All of the t-values for the Bone Mineral Analyzer comparisons ($t = 1.887$ to -2.696) were significant at the 5% level or better, while the t-value for the S.E.D. comparison ($t = 0.451$) was not at all significant. The conclusion is that radial metaphyseal S.E.D. measurements cannot distinguish between even grossly different clinical groups, although this may stand to reason if trabecular bone density is a constant in disease as it apparently is with age in normals (Exner-1979).

This comparative study of the efficancy of the Norland-Cameron Bone Mineral Analyzer and the A.E.C.L. Bone Densitometer as monitors of bone mineral status in various clinical conditions involving metabolic bone disease clearly shows the inferiority of the Bone Densitometer to this purpose. Neither increases nor decreases in skeletal mineralization with age have been demonstrated with consistency, and

no difference can be detected between mean values in even such diverse clinical groups as post-menopausal osteoporosis and hypoparathyroidism. The fault is not that the Bone Densitometer does not give an index of trabecular bone density, but rather, that trabecular bone density probably does not change sufficiently with age of disease in the clinically important cases.

TABLE 6.2 Statistical data on bone mineral measurements in three clinical groups of adult females.

GROUP	N	DISTAL RADIAL METAPHYSIS S.E.D.	1/3 DISTAL RADIUS		1/10 DISTAL RADIUS	
			BMC (g/cm)	BMC/BW (g/cm^2)	BMC (g/cm)	BMC/BW (g/cm^2)
Rheumatoid Arthritis	12	1.092 (0.061)	0.698g (0.102)	0.540 (0.096)	0.668 (0.111)	0.388 (0.062)
Post-Menopausal Osteoporosis	9	1.131 (0.007)	0.644 (0.235)	0.495 (0.169)	0.583 (0.297)	0.352 (0.158)
Hypoparathyroid	5	1.146 (0.041)	0.849 (0.058)	0.704 (0.029)	0.880 (0.098)	0.497 (0.028)

Values in brackets are standard deviations.

TABLE 6.3 Comparison of group mean values of bone mineral indices for two groups of adult females. One group had post-menopausal osteoporosis and the other group had hypoparathyroidism.

	DISTAL RADIAL METAPHYSIS	1/3 DISTAL RADIUS		1/10 DISTAL RADIU	
	S.E.D.	BMC	BMC/BW	BMC	BMC/BW
t-value	-0.451	-1.887	-2.696	-2.138	-1.999
degrees of freedom	12	12	12	12	12

7. Evaluation of the A.E.C.L. Bone Densitometer As An Instrument For In Vivo Monitoring of Skeletal Mineralization.

The A.E.C.L. Bone Densitometer is a prototype instrument intended for in vivo monitoring of skeletal mineralization as an aid to diagnosis and treatment of metabolic bone disease. Since changes in skeletal mineralization appear earliest, and are most pronounced, at sites of cancellous bone (Dalén-1973), the Bone Densitometer was designed to measure the density of a small volume of trabecular bone at any convenient site in the appendicular skeleton. If several theoretical assumptions could be met in this intended application, the measurement would be independent of surrounding cortical bone and soft tissue cover. Actually the Densitometer measures specific electron density (S.E.D.) in principle, but, since S.E.D. is closely related to physical density, a satisfactory index of trabecular bone mineral status would still result. It is the purpose of this thesis to assess the A.E.C.L. Bone Densitometer as a clinically useful instrument for monitoring skeletal mineral status.

Three levels of experimentation were undertaken to assess the Bone Densitometer. First, the instruments accuracy and precision in measuring the density of homogeneous samples of matter under various geometric conditions was in-

vestigated. Then, in vitro measurements on excised cadaver bones were performed at sites of trabecular bone formation to determine whether S.E.D. measurements truly reflected the amount of bone mineral present. Finally, a series of in vivo measurements were made on a number of patients with metabolic bone disease to evaluate the Bone Densitometer under clinical conditions. The results these experiments are summarized below.

Specific electron density (S.E.D.) measurements on homogeneous samples with standardized geometries were in good agreement with expected values. S.E.D. measurements on cylindrical vials of various solutions, and on cylindrical lucite and aluminum phantoms, correlated well ($r = 0.996$, $N = 12$) with S.E.D. values calculated for these substances, and also with their physical densities ($r = 0.998$, $N = 12$). The ranges of calculated S.E.D. and physical density covered were 0.79 to 2.35 and 0.79g/cm^3 to 2.74g/cm^3 respectively.

However, the measured S.E.D. value for a given substance was demonstrated to be geometry dependent, and the degree of dependence was a function of the S.E.D. of the substance. When a cylinder of lucite of density 1.20g/cm^3 was positioned in various orientations, S.E.D. measurements

varied by as much as 3%. Similar measurements on an Aluminum cylinder of density 2.74g/cm^3 varied by about 8%.

The effect of surrounding material on the S.E.D. measurement at and around a point was found to depend a great deal on the circumstances obtaining. Firstly, since the S.E.D. measurement is an average over a finite volume around the point of measurement, any surrounding material which encroached on the boundary of this volume affected the result. Secondly, if surrounding material was not both homogeneous and symmetrically distributed, an erroneous S.E.D. value resulted. Thirdly, the dimensions of the volume being measured were shown to increase somewhat as the density of the material being measured increased. Consequently, the magnitude of the error in measured S.E.D. introduced by surrounding material is variable, and not readily specified by any one value.

Repeated measurements on cylindrical lucite and aluminum phantoms were made to test the reproducibility of S.E.D. measurements under standard conditions. The coefficient of variation of the lucite phantom S.E.D. values was calculated for monthly intervals and ranged from 1.0% (N = 8) to 3.2% (N = 4). Twenty-two S.E.D. measurements made on the lucite phantom over a nineteen day period had a coefficient of variation of 2.5%.

The accuracy with which the A.E.C.L. Bone Densitometer can measure trabecular bone mineralization was investigated by making in vitro specific electron density (S.E.D.) measurements of excised cadaver bone specimens, and comparing the results to ash weights of the specimens. S.E.D. measurements were made at trabecular sites in twenty capitates, twenty radii, twenty thoracic vertebrae, ten tibial and ten femora. Fifty of the bone specimens were measured before and after defatting by boiling. The S.E.D. measurements were compared to the ash density (weight of a $0.3cm^3$ cylindrical volume of cancellous bone) at the point of S.E.D. measurement in each bone specimen, except in the case of the capitates, which were ashed whole. Parallel bone mineral measurements were made at the same site using a well-established photon absorptiometric method (Cameron-1963) as an additional standard for comparison. These measurements were made with a Norland-Cameron Bone Mineral Analyzer and were compared to ash weights of 1cm long slices cut from the measurement sites.

Correlations between specific electron density (S.E.D.) after defatting and ash density ranged from poor ($r = 0.507$, $N = 10$) to good ($r = 0.947$, $N = 9$) when each

type of bone was taken separately as a group. The correlation was only moderate ($r = 0.632$, $N = 56$) when all bones, excluding the capitates, were taken together. Although some of the lack of correlation may be accounted for by the different shape and size of the S.E.D. measurement volume (about $4cm^3$, and diamond-shaped in corss-section), the variation in bone morphology must also have been a factor. In the case of the smaller bones, such as the vertebrae and capitates, some of the surrounding cortical bones, and/or some of the water cover, might inadvertently have been included within the elongated S.E.D. measurement volume (long axis about 4cm).

In contrast, the Bone Mineral Analyzer (BMA) measurements of bone mineral content (BMC) correlated very highly with the ash weights of the bone slices. When each bone type was considered individually, correlation coefficients ranged from $r = 0.915$, $N = 10$ to $r = 0.988$, $N = 9$, and when taken all together, excluding the capitates, the correlation coefficient was $r = 0.986$, $N = 56$.

Comparing specific electron density measurements before boiling to those after boiling gives a measure of the error introduced by trabecular marrow fat. Pre-boiling measurements were on the average 7% lower than post-boiling values. An elementary analysis indicates that an error of

this magnitude would occur if trabecular bone were decreased by 50% and 85% of cell water were replaced by fat.

Bone Mineral Analyzer measurements were on the average 10% lower before boiling than after boiling, indicating that measurement of a trabecular site by the photon absorptiometric method would also be compromised by fatty marrow.

Two in vivo studies were performed to evaluate the Bone Densitometer's usefulness in clinical situations. In one study, the tibial bone mineral status and rate of growth of a group of paraplegic children undergoing standing therapy was compared to those of a group of age-matched normal children. The Bone Mineral Analyzer measurements indicated that the paraplegic group had significantly less tibial bone development (0.79% increase in bone mineral content (BMC) per month of age) prior to standing therapy than the normal group (1.50% increase in BMC per month of age). The rate of BMC increase in the paraplegic group over the period of standing therapy was 1.53%. Parallel specific electron density measurements in the paraplegic group showed a rate of change in tibial trabecular bone density of -0.11% per month of age prior to therapy and of +0.25% per month during therapy.

In the other clinical study, the radial bone min-

eral status of three groups of adult females with diagnosed metabolic bone disease was investigated using both the Bone Mineral Analyzer (BMA) and the Bone Densitometer. BMA measurements indicated age-related bone mineral changes which were in agreement with the clinical picture, while the Bone Densitometer measurements of specific electron density (S.E.D.) did not. Nor did the S.E.D. measurement distinguish between group means on the basis of a t-test as did the BMA measurements.

On the basis of the foregoing evidence, it is apparent that the A.E.C.L. Bone Densitometer is not a clinically useful instrument for the diagnosis or medical follow-up in cases of metabolic bone disease. While it is true that the specific electron density (S.E.D.) measurements it provides correlate well with physical density under very standardized conditions, S.E.D. measurements are subject to error due to amount, nonhomogeneity and asymmetry of material surrounding the point of S.E.D. measurement. In vitro specific electron density measurements of trabecular bone specimens correlate only moderately well with the concentration trabecular bone present at the S.E.D. measurement site, primarily due to the fact that the physical density of cancellous bone would only decrease from the normal value of

1.09g/cm^3 to a value of 1.04g/cm^3 if all of the trabecular bone was resorbed! Further, since a 20% by volume replacement of water by fat in cancellous bone marrow causes the about the same decrease in cancellous bone density as a 30% decrease in trabeculation, in vivo monitoring of trabecular bone sites with the A.E.C.L. Bone Densitometer to detect small percentages of demineralization would seem fruitless! Clinical studies have proved this to be the case.

BIBLIOGRAPHY

Blanton, P.L. and N.L. Biggs, "Density of Fresh and Embalmed Human Compact and Cancellous Bone", American Journal of Anthropology, 29: 39-44, (1968).

Clarke, R.L. and G. VanDyk, "A New Method for Measurement of Bone Mineral Content Using Both Transmitted and Scattered Beams of Gamma-Rays", Journal of Physics, Medicine, and Biology, Vol. 18, No. 4, 532-539 (1973).

Dalén, N, "Bone Mineral Assay-Choice of Measuring Sites", International Conference on Bone Mineral Measurement, U.S. DHEW No. (N1H) 75-683, (1973).

Dalén, N. and B. Jacobson, "Bone Mineral Assay-Choice of Measuring Sites", Investigate Radiology, 9: 174-185 (1973).

Exner, G.U. and A. Prader, "Bone Densitometry Using Computed Tomography", Part 1: Selective Determination of Trabecular Bone Density and other bone mineral parameters, Normal values in children and adults, British Journal of Radiology, 52, 14-23 (1979).

GARNETT, E.S. and T.J. Kennett, D.B. Kenyon, C.E. Webber, "A Photon Scattering Technique for the Measurement of Absolute Bone Density in Man", Radiology 106: 209-212, January 1973.

Goldsmith, N.F. and J.O. Johnston, H. Ury, G. Vose, C. Colbert, "Bone Mineral Estimation in Normal and Osteoporotic Women. A comparability trial of four methods and seven bone sites", The Journal of Bone and Joint Surgery, Vol. 53-A, No. 1, pp. 83-100, January 1971.

Goldsmith, N.F., "Normative Data From the Osteroporosis Prevalence Survey, Oakland, California, 1969-1970. Bone Mineral at the Distal Radius: Variation with age, sex, skin color, and exposure to oral contraceptives and exogeneous hormones; relation to Aortic calcification, Osteoporosis, and Hearing loss". International Conference on Bone Mineral Measurement, U.S. DHEW No. (N1H) 75-683, (1973).

Griffiths, H.J., R.E. Zimmerman, "An Overview of Clinical Application of Photon Absorptiometry", American Journal of Roentgenology, Radium Therapy, and Nuclear Medicine, Vol. 126, No. 6, June, 1976.

Hazan, G. and I. Leichter, E. Loewinger, A. Weinreb, G.C. Robin, "The Early Detection of Osteoporosis by Compton Gamma Ray Spectroscopy", Phys. Med. Biol., Vol.22, No. 6, 1073-1084 (1977)

Jacobson, B. "X-ray Spectrophotometry In Vivo", American Journal Roentgenology, 91: 202-210, (1964).

Johnston, J.O. and N.F. Goldsmith, "A Clinical Trial of the I-125 Isotope Scanning Device as a Screening Method for the Early Detection of Osteoporosis", Proceedings of Bone Measurement Conference, U.S.A.E.C. Conf. 700515, pp. 340-346, (1970).

Kan, W.C., C.R. Wilson, R.M. Witt, R.B. Mazess, "Direct Read-out of Bone Mineral Content with Dichromatic Absorptiometry", International Conference on Bone Mineral Measurement, U.S. DHEW No. (NIH) 75-683, (1973).

Kennett, T.J., and C.E. Webber, "Bone Density Measured by Photon Scattering. II. Inherent Sources of Error", Phys. Med. Biol., 1976, Vol. 21, No. 5, 770-780.

Klemm, T. and D.H. Banzer, U. Schneider, "Bone Mineral Content of the Growing Skeleton", The American Journal of Roentgenology, Radium Therapy and Nuclear Medicine, Vol. 126, No. 6, June 1976.

Lachman E., "Osteoporosis: Potentialities and Limitations of Its Roentgenologic Diagnosis". Amer. J. Roentgen., 74: 712-715, 1955.

Luther, R., "Correlation of Os Calcis and Spinal Bone by Compton Scattering", International Conference on Bone Mineral Measurement, U.S. DHEW No. (NIH) 75-683, (1973).

Manzke, C.H.C. III, J.E. Wergedal, D.J. Baylink, W.B. Nelp, "Relationship Between Local and Total Bone Mass in Osteoporosis", J. Nuc. Med., 15: 428-435, 1974.

Mazess, R.B. and J.R. Cameron, "Bone Mineral Content in Normal U.S. Whites", International Conference on Bone Mineral Measurement, U.S. DHEW No.(NIH), 75-683, (1973).

Mazess, R.B. and M.G. Ort, P.F. Judy, W. Mather, "Absorptiometric Bone Mineralization Determination Using ^{153}Gd", Proceedings of Bone Measurement Conference, U.S.A.E.C. Conf. 700515 pp. 308-312, (1970).

Mueller, M.N., "Effects of Corticostersids on Bone Mineral in Rheumatoid Arthritis and Asthma", Proceedings of the Symposium on Bone Mineral Determination, Stockholm, Studsvik, p. 1300, A.E.-489, Vol. 1, (1974).

Mueller, M.N. and R.B. Mazess, J.R. Cameron, "Corticosteroid Therapy Accelerated Osteoporosis in Rheumatoid Arthritis", International Conference on Bone Mineral Measurement, Chicago, Illinois, DHEW No. (N1H) 75-683 (1973).

Nilsson, B.E. and N.E. Westlin, "Bone Mass and Colle's Fracture", International Conference on Bone Mineral Measurement, Chicago, Illinois, DHEW No. (N1H) 75-683 pp. 362-368, (1973).

Panel Discussion, "Measuring Sites", pp.190-193, Proceedings of the Symposium on Bone Mineral Determination, Stockholm, Studsvik, 1974, AE-489, Vol. 2.

Reiss, K.H. and B. Steinke, "Medical Application of the Compton Effect", Seimens Forsch. U. Entwickle Berichte, Bd. 2, Nr. 1, Springer-Uerlag, Berlin, Germany, (1973).

Schlenker, R.A., "Percentages of Cortical and Trabecular Bone Mineral Mass in the Radius and Ulna", The American Journal of Roentgenology, Radium Therapy, and Nuclear Medicine, Vol. 126, No. 6, June 1976.

Schlenker, R.A. and B.G. Oltman, "Effects of Skeletal Radium Deposits on Bone Mineralization", International Conference on Bone Mineral Measurement, Chicago, Illinois, DHEW No. (N1H) 75-683, (1973).

Schneider, U. and D. Banzer, M. Gange, "Comparison of Bone Mineral Content (BMC) in Different Skeletal Sites", Amer. J. Roentgenol., Radium Therapy, and Nuclear Medicine, Vol. 126, No. 6, pp. 1312-1313, June 1976.

Shapiro, J.R. and W.T. Moore, H. Jorgenson, C. Epps, J. Reid, G.D. Whedon, "A Preliminary Evaluation of Diagnosis and Therapy in Osteoporosis", International Conference on Bone Mineral Measurement, Chicago, Illinois, DHEW No. (N1H) 75-683, 1973.

Shimmins, J., J.B. Anderson, D.A. Smith, and M. Aitken, "The Accuracy and Reproducibility of Bone Mineral Measurements 'In Vivo' (a) The Measurement of Metacarpal Mineralization Using an X-ray generator". Clin Radiol (1972) 23, 42-46.

Singh, M., A.R. Nagrath, P.S. Maimi, "Changes in Trabecular Pattern of the Upper End of the Femur as an Index of Osteoporosis", Journal of Bone and Joint Surgery, 53-A: 457-467, (1970).

Smith, D.M. and C.C. Johnston, Pao-Yu, "In Vivo Measurement of Bone Mass: Its Use in Demineralized States Such as Osteoporosis", Jama, Jan. 17, 1972, Vol. 219, No. 3.

Smith, D.M. and C.C. Johnston, Pao-Lo Yu, "Bone Mass In The Radius, A Reflection of the Axial Skeleton", Proceedings of Bone Measurement Conference, pp. 398-404, U.S.A.E.C. Conf. - 700515, 1970.

Smith, D.M. and M.R.A. Khairi, C.C. Johnston, "Mineral Loss With Aging Measured Prospectively by the Photon Absorption Technique", International Conference on Bone Mineral Measurement, Chicago, Illinois, DHEW No. (N1H) 75-683, 1973.

Sokal, R.R. and F.J. Rohlf, "Introduction to Biostatistics", W.H. Freeman and Co., 1973.

Sorenson, J.A. and R.B. Mazess, "Effects of Fat on Bone Mineral Measurements", International Conference on Bone Mineral Measurement, Chicago, Illinois, DHEW No. (N1H) 75-683, 1973.

Trotter, M. and G. Broman, R. Peterson, "Densities of Bones of White and Negro Skeletons", J. Bone Jt. Surgery 42-A, No. 1, pp. 50-58, 1960.

Webber, C.E. and T.J. Kennett, "Bone Density Measured by Photon Scattering",
I. A System For Clinical Use, Phys. Med. Biol. 1976, Vol. 21, No. 5, 760-769, 1976.

Wilson, C.R., "The Use of In Vivo Bone Mineral Determination to Predict the Strength of Bone", Ph. D Thesis, University of Wisconsin, 1972.

Wilson, C.R., "Prediction of Femoral Neck and Spine Bone Mineral Content from the BMC of the Radius or Ulna and the Relationship Between Bone Strength and BMC", International Conference on Bone Mineral Measurement, (Mazess, R.B. Ed.) pp, 51-60, Washington, U.S. DHEW No. (N1H) 75-683, 1973.

Wing, K., "Panel Discussion-Measuring Sites", Proceedings of the Symposium on Bone Mineral Determination, Stockholm, Studsuik, pp. 192-193, 1974.

Witt, R.M. and R.B. Mazess, J.R. Cameron, "Standardization of Bone Mineral Measurements", Proceedings of Bone Measurement Conference, Chicago, Illinois, U.S. AEC Conf.-700515, 1970.

Wooten, W.W. and P.F. Judy, M.A. Greenfield, "Analysis of the Effects of Adipose Tissue on the Absorptiometric Measurement of Bone Mineral Mass", Invest-Radiol. 8: 84-89, 1973.

Zimmerman, R.E. and H.J. Griffiths, P. Pletka, D. Bernstein, "Absolute Calibrations of a ^{125}I Bone Absorptiometry System", Proceedings of the Symposium on Bone Mineral Determinations, Stockholm, Studsuik, 1974, AE-489, Vol. 1.

Acknowledgements

I would like to express my sincere appreciation to Dr. J.B. Sutherland for his perpetual encouragement throughout my graduate studies at the University of Manitoba, and for his considerable role in initiating and supporting the work of this thesis.

I would also like to thank Dr. Douglas Cormack for his incisive objectivity, Dr. W. James Dubé for his organization of the clinical studies, and Dr. Paul Major for his understanding.

I am also grateful to the following individuals: Dr. Richard Mark, Dr. Graham Matthews, and Dr. Allen Wright for their assistance in excising the cadaver bones; Dr. F.D. Baragar, Dr. Chas. Hollenberg, and Dr. R.M. Letts for their cooperation in the clinical studies; Larry Bluhm and Dave Maughan for cutting the bone sections; Jules Legal, his staff for their collective machinist wizardry; Vivian Wilkes for her help with the clinical measurements; and Carol Sproule for her heroic job of typing the manuscript.